AD-A087 274 AIR FORCE WRIGHT AERONAUTICAL LABS WRIGHT-PATTERSON AFB OH F/G 16/4
TEST OF AN ELECTROHYDRAULIC DIGITAL ACTUATOR FOR ADVANCED MISSI--ETC(U)
FEB 80 M C TWYMAN

UNCLASSIFIED AFWAL-TR-80-2001 NL

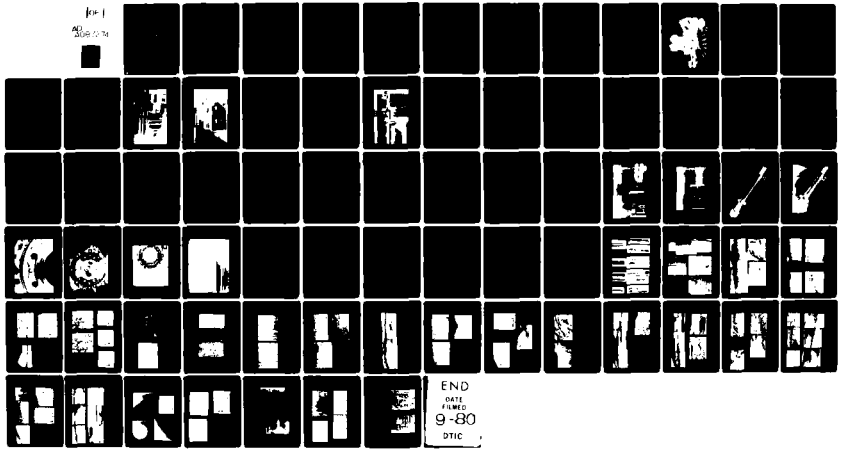

END
DATE FILMED
9-80
DTIC

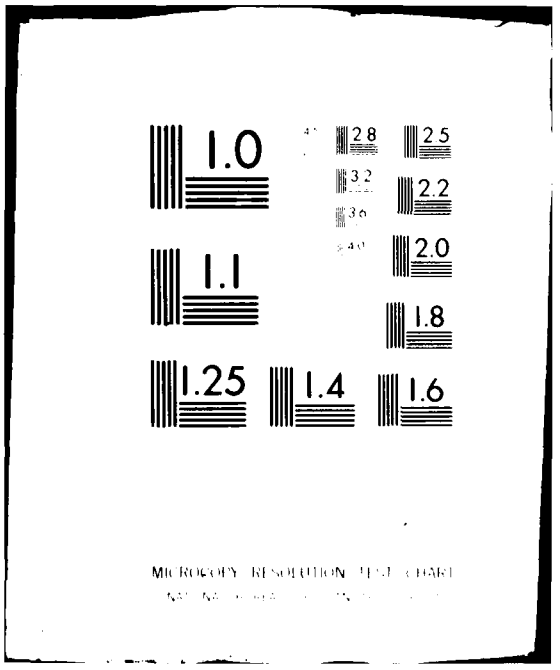
1.0
2.8
2.5
3.2
2.2
3.6
2.0
1.1
1.8
1.25
1.4
1.6
MICROCOPY RESOLUTION TEST CHART

AFWAL-TR-80-2001

LEVEL II

(2)

TEST OF AN ELECTROHYDRAULIC DIGITAL ACTUATOR FOR ADVANCED MISSILE SYSTEMS

Power Systems Branch
Aerospace Power Division

February 1980

TECHNICAL REPORT AFWAL-TR-80-2001

Final Report for Period September 1978 - September 1979

Approved for public release; distribution unlimited.

AERO PROPULSION LABORATORY
AIR FORCE WRIGHT AERONAUTICAL LABORATORIES
AIR FORCE SYSTEMS COMMAND
WRIGHT-PATTERSON AIR FORCE BASE, OHIO 45433

NOTICE

When Government drawings, specifications, or other data are used for any purpose other than in connection with a definitely related Government procurement operation, the United States Government thereby incurs no responsibility nor any obligation whatsoever; and the fact that the government may have formulated, furnished, or in any way supplied the said drawings, specifications, or other data, is not to be regarded by implication or otherwise as in any manner licensing the holder or any other person or corporation, or conveying any rights or permission to manufacture, use, or sell any patented invention that may in any way be related thereto.

This report has been reviewed by the Information Office (OI) and is releasable to the National Technical Information Service (NTIS). At NTIS, it will be available to the general public, including foreign nations.

This technical report has been reviewed and is approved for publication.

C. Mark Twyman

MARK C. TWYMAN
Project Engineer
Power Systems Branch

B L McFadden

B. L. MCFADDEN
Acting Chief
Power Systems Branch

FOR THE COMMANDER

J D Reams

JAMES D. REAMS
Chief, Aerospace Power Division
Aero Propulsion Laboratory

"If your address has changed, if you wish to be removed from our mailing list, or if the addressee is no longer employed by your organization please notify AFWAL/POOS *,W-PAFB, OH 45433 to help us maintain a current mailing list".*

Copies of this report should not be returned unless return is required by security considerations, contractual obligations, or notice on a specific document.

AIR FORCE/56780/9 July 1980 — 100

SECURITY CLASSIFICATION OF THIS PAGE *(When Data Entered)*

REPORT DOCUMENTATION PAGE

READ INSTRUCTIONS BEFORE COMPLETING FORM

1. REPORT NUMBER: AFWAL-TR-80-2001	2. GOVT ACCESSION NO.: AD-A087274
3. RECIPIENT'S CATALOG NUMBER:	
4. TITLE *(and Subtitle)*: TEST OF AN ELECTROHYDRAULIC DIGITAL ACTUATOR FOR ADVANCED MISSILE SYSTEMS	5. TYPE OF REPORT & PERIOD COVERED: Final Report Sept 1978 - Sept 1979
	6. PERFORMING ORG. REPORT NUMBER:
7. AUTHOR(s): Mark Twyman	8. CONTRACT OR GRANT NUMBER(s): 3145
9. PERFORMING ORGANIZATION NAME AND ADDRESS: Aero Propulsion Laboratory (POOS) AF Wright Aeronautical Laboratories, AFSC Wright-Patterson Air Force Base, Ohio 45433	10. PROGRAM ELEMENT, PROJECT, TASK AREA & WORK UNIT NUMBERS: Program Element 62203F Project 3145, Task 314530, Work Unit 31453021
11. CONTROLLING OFFICE NAME AND ADDRESS: Aero Propulsion Laboratory (POO) AF Wright Aeronautical Laboratories, AFSC Wright-Patterson Air Force Base, Ohio 45433	12. REPORT DATE: February 1980 13. NUMBER OF PAGES: 78
14. MONITORING AGENCY NAME & ADDRESS *(if different from Controlling Office)*	15. SECURITY CLASS. *(of this report)*: Unclassified 15a. DECLASSIFICATION/DOWNGRADING SCHEDULE

16. DISTRIBUTION STATEMENT *(of this Report)*

Approved for public release; distribution unlimited.

17. DISTRIBUTION STATEMENT *(of the abstract entered in Block 20, if different from Report)*

18. SUPPLEMENTARY NOTES

19. KEY WORDS *(Continue on reverse side if necessary and identify by block number)*

Digital actuator
Dynavector
Hydraulic motor
Missile system actuator

20. ABSTRACT *(Continue on reverse side if necessary and identify by block number)*

This report describes the testing of a digital electrohydraulic stepper actuator developed by Bendix Systems Division under a previous Air Force R&D contract. The testing included calibration and 50 hours of durability cycling type tests. The actuator was designed for a stall torque of 2000-inch pounds at a 3000 psi differential pressure. A discussion of the problems encountered during this program and an inspection analysis of the actuator after testing are included in this report.

DD FORM 1 JAN 73 1473 EDITION OF 1 NOV 65 IS OBSOLETE

SECURITY CLASSIFICATION OF THIS PAGE *(When Data Entered)*

JOB

FOREWORD

This report contains the results from tests conducted on an Electrohydraulic Digital Actuator. The work was performed in the Power Systems Branch (POOS), Aerospace Power Division (POO), Aero Propulsion Laboratory, Air Force Wright Aeronautical Laboratories, Wright-Patterson Air Force Base, Ohio, under Project 3145, Task 314530, "Fluid Power," Work Unit 31453021, "Fluid & Mechanical Power Technology Demonstration."

The work was conducted by Mr Mark Twyman during the period, January 1979 to March 1979. This in-house test was conducted in order to verify test results received from the Bendix Corporation.

Special acknowledgment is given to Mr Harold Lee for his generous support and assistance; also Mr Kenneth Binns for his excellent technical consultation during this program. The contributions to this program of L. F. Mayer, Jack Silvius of Bendix Aerospace Division, and Kamal E. Amin of Bendix Research Laboratories are hereby acknowledged with appreciation.

TABLE OF CONTENTS

LIST OF ILLUSTRATIONS

LIST OF ILLUSTRATIONS (CONTINUED)

SECTION I

INTRODUCTION

The Bendix Aerospace Corporation previously developed an electro-hydraulic digital actuator under Contract F33615-74-C-2052 (Reference 1). A mechanical failure (reaction pin spacer) of a prototype actuator abbreviated the testing during the Bendix program. A potential solution was determined by Bendix and the prototype actuator was reworked with new parts. The purpose of this program was to repeat the durability test of this actuator to verify the actuator redesign.

The actuator characteristics used for design purposes and the performance demonstrated by Bendix are shown in Table 1. These characteristics were based on preliminary ASALM missile requirements. This actuator concept combines a high speed orbiting motor with a high-ratio transmission to provide high torque, low speed rotary power. The control surface is moved in discrete steps by electrohydraulic valves that respond to digital input commands. The time required for the actuator to move one degree in response to one command is 0.005 to 0.007 seconds. The three major components of the actuator system are the motor, an integral transmission, and the first stage control valves. These are shown in Figures 1 and 2.

1. ACTUATOR MOTOR

The actuator motor is the power element or second stage of the system. It consists of a positive displacement, very low inertia, non-rotating vane motor. Its output is a radial force which can be rotated at commanded stepping speeds in either direction of rotation. The displacement chambers (Figure 1) formed by the vanes and housing expand and collapse at the same speed as the force vector but do not rotate.

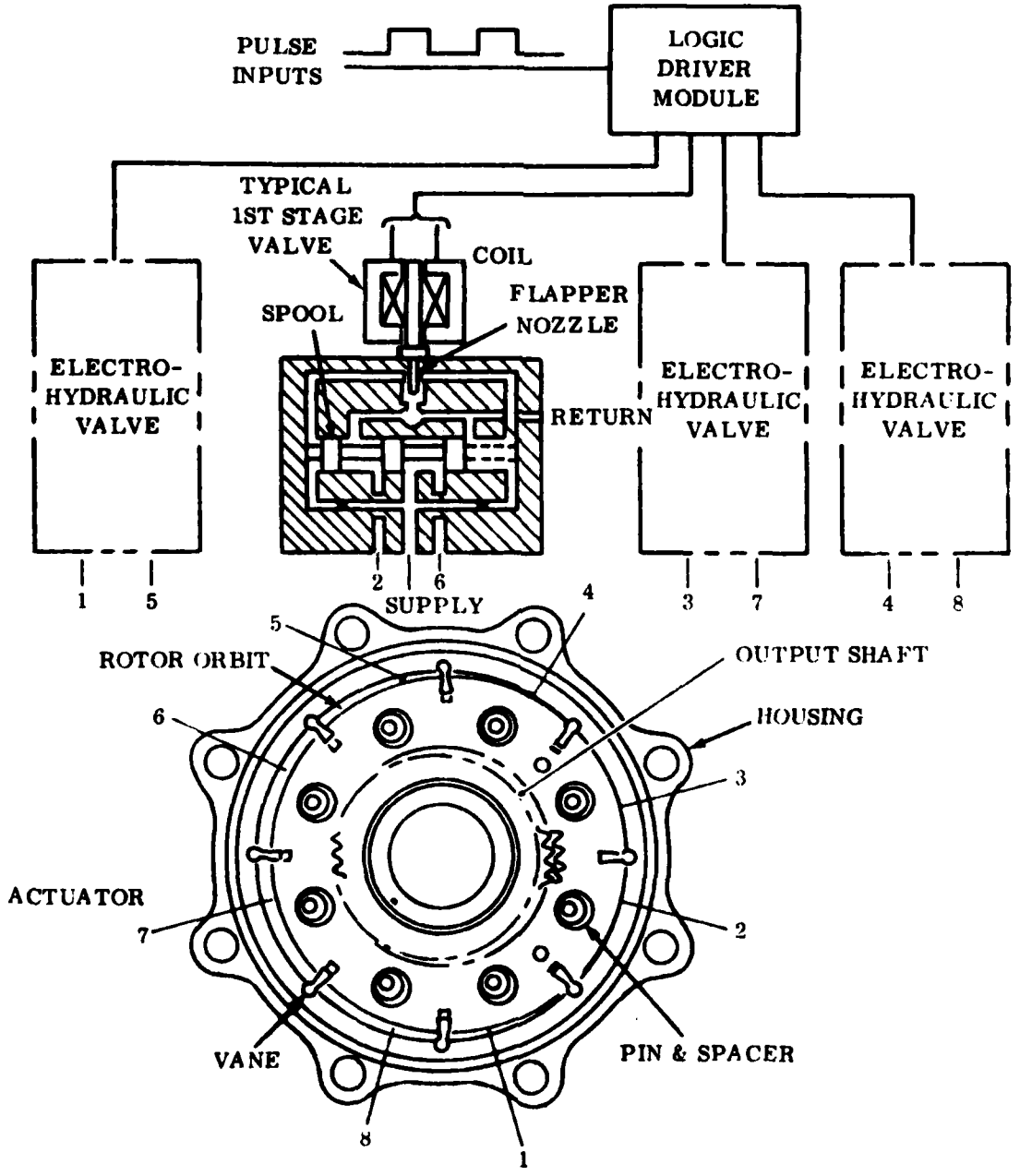

*Figure 1. Actuator System Schematic

*Numbers 1-8 Indicate Motor Chambers

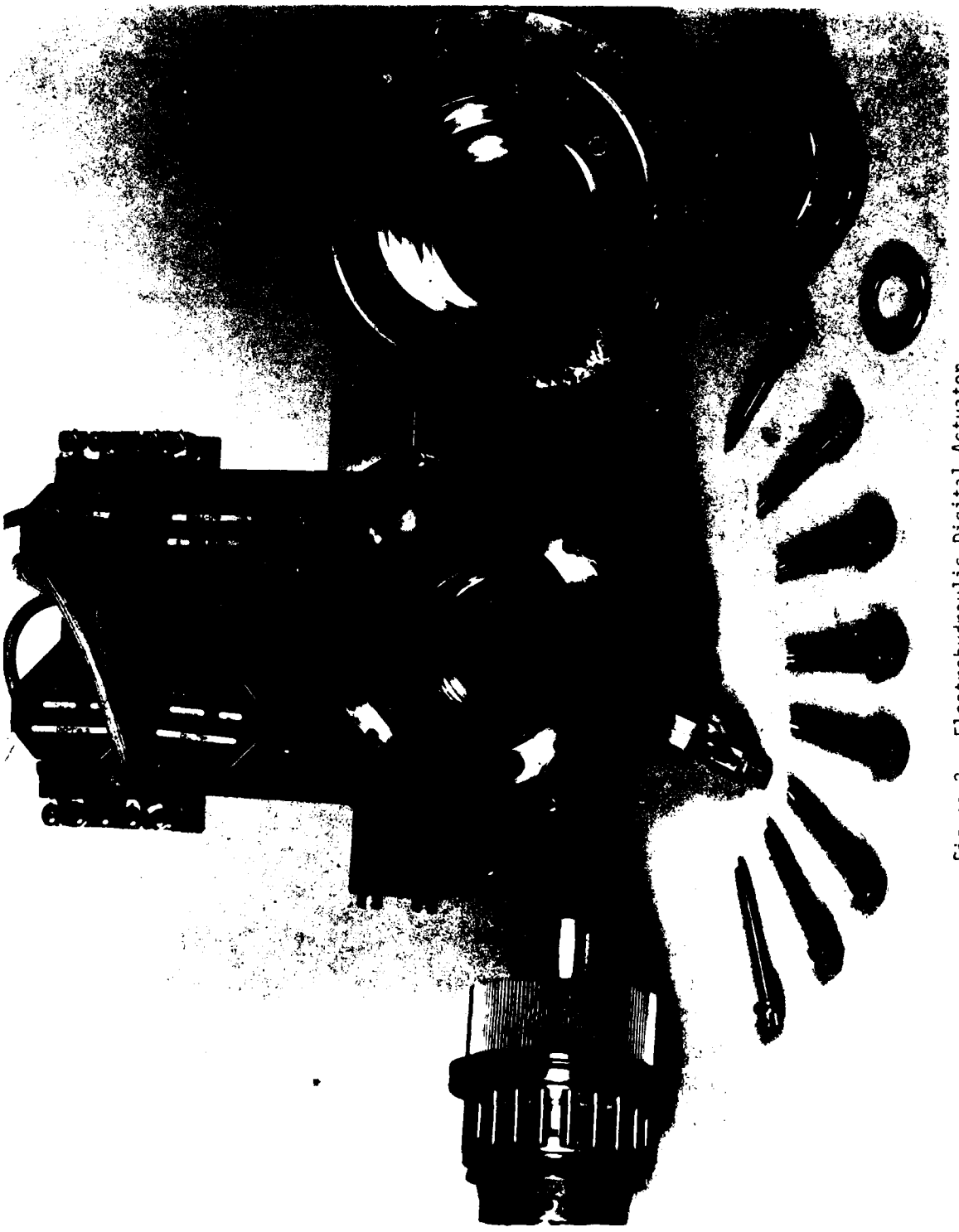

Figure 2. Electrohydraulic Digital Actuator (Exploded View)

The direction of the force vector is established by applying supply pressure to four adjacent displacement chambers (for example, 1, 2, 3, 4) while venting the other four chambers (5, 6, 7, 8) to drain pressure. The force vector is rotated one "step" (or 45 degrees) by then pressurizing the proper vented chamber (for example, 5) while concurrently venting the opposing pressurized chamber (1). The actuator may be rotated through a single step while operating in the open loop mode by applying a single digital input pulse, or it may be rapidly rotated through a series of steps by applying a chain of digital pulses and will stop at the preselected position.

2. TRANSMISSION

The transmission consists of an internal spur gear which is integral with the orbiting rotor of the actuator motor, and a mating external spur gear on the output shaft. The driving gear does not rotate but orbits about a small radius of eccentricity to drive the output gear. The eccentricity is controlled by the clearance between the reaction pin and the holes through the rotor. As suggested by their name, the reaction pins provide the rotor reaction force. The transmission ratio is given as:

$$R_t = \frac{N_o}{N_o - N_i} = \frac{135}{138-135} = 45$$

where R_t = transmission ratio

R_o = number of teeth on output gear

N_i = number of teeth on input gear

Thus, one stop of the orbiting rotor (45 degrees) will rotate the output shaft one degree. Analysis of the multipurpose missile control loop indicated that an output shaft resolution of one degree is satisfactory for missile control, so the actuator was designed to provide this resolution.

This transmission design provides an input gear pitch diameter which is only slightly larger than the output gear pitch diameter. Thus, a slight gear tooth deflection under load allows many gear teeth to share the load. This same feature provides high resistance to shock overload and minimizes dynamic loading forces. The transmission has excellent torque transmitting capability because the dynamic tooth loads are negligible so that the dynamic strength is nearly equal to the static strength.

3. CONTROL VALVES

The eight displacement chambers of the actuator motor are controlled by four electrohydraulic servovalves. Each valve is connected to two diametrically opposed chambers so that when one chamber is connected to supply pressure, the other is connected to drain pressure. A modified Moog Type 30 servovalve was selected for this application. The stepper controller is designed to step the valves sequentially, as shown in Table 1 for clockwise rotation of the actuator. The stepping sequence is reversed for counterclockwise rotation.

TABLE 1

STEPPING SEQUENCE

Step	Valves Energized	Chambers Pressurized
0 CW	3, 4	7, 8, 1, 2
1 CW	4	8, 1, 2, 3
2 CW		1, 2, 3, 4
3 CW	1	2, 3, 4, 5
4 CW	1, 2	3, 4, 5, 6
5 CW	1, 2, 3	4, 5, 6, 7
6 CW	1, 2, 3, 4	5, 6, 7, 8
7 CW	2, 3, 4	6, 7, 8, 1
8 CW	3, 4	7, 8, 1, 2

SECTION II

DESCRIPTION OF TEST RIG

All tests were performed within the AFWAL Fluid Power Laboratory. A schematic of the test rig is shown in Figure 3. The Laboratory test rig is shown in Figure 4.

Two pieces of equipment were designed by Bendix Corporation specifically for use in this actuator program; a Dynavector Control Chassis, and a Dynavector Test Adapter.

The Dynavector Control Chassis (Figure 5) receives, from an external frequency generator, a square wave signal and then provides the electric pulses to the control valves of the actuator. The Control Chassis is designed for two modes of operation, manual or automatic. In the manual mode, the actuator is advanced one step at a time by pressing a step button. The direction of rotation is controlled by a switch. The automatic mode will allow the actuator to run in a continuous loop or in a cycle, with the use of a built-in limit switch, between selected shaft positions. Commanded shaft positions are indicated on the control panel by a digital readout.

The Dynavector Test Adapter transmits torque and inertia loads to the actuator. The torque is developed with a torsion spring rated at 2000 inch pounds at 30° deflection. A calibration of the spring is shown in Figure 6. Inertia plates can be installed on the adapter to evaluate the effects of different amounts of inertia applied to the actuator. The basic fixture has an inertia of 0.11 inch pounds/sec^2, and each plate has an inertia of 0.32 inch pounds/sec^2.

The adapter utilizes a Lebou No. 1204-200 torque sensor between the actuator and load. A visual position indicator shows the actual position, in degrees, of the actuator shaft. The test stand is shown in Figures 7 and 8.

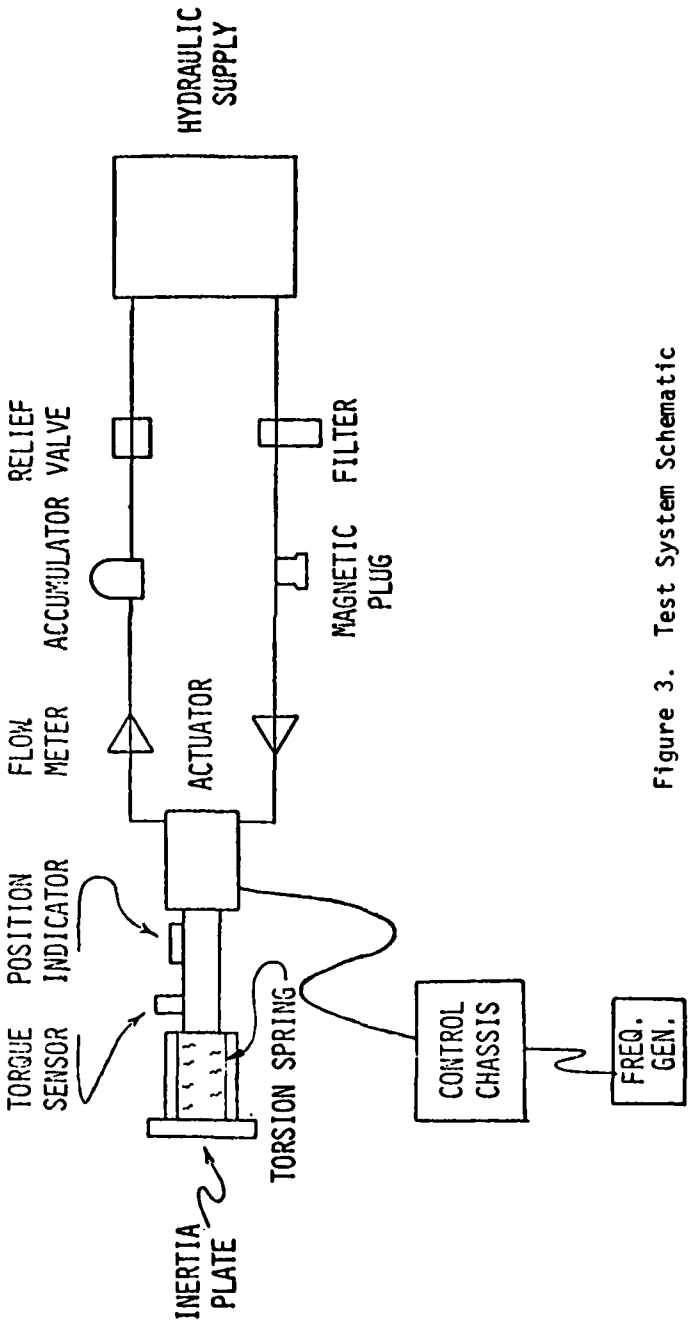

Figure 3. Test System Schematic

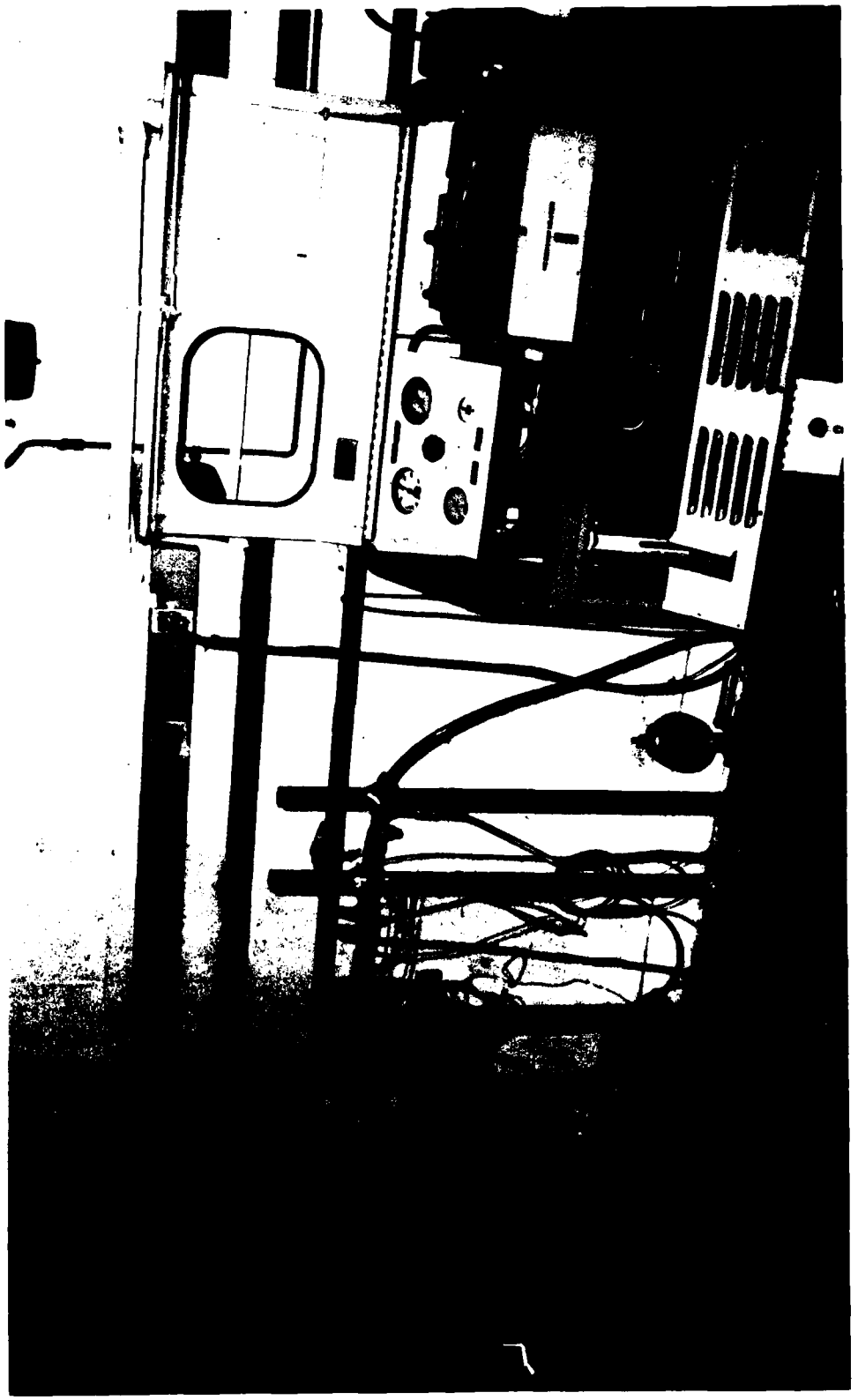

Figure 4. Actuator Test Stand
(Power Supply, Actuator, and Torque Sensor)

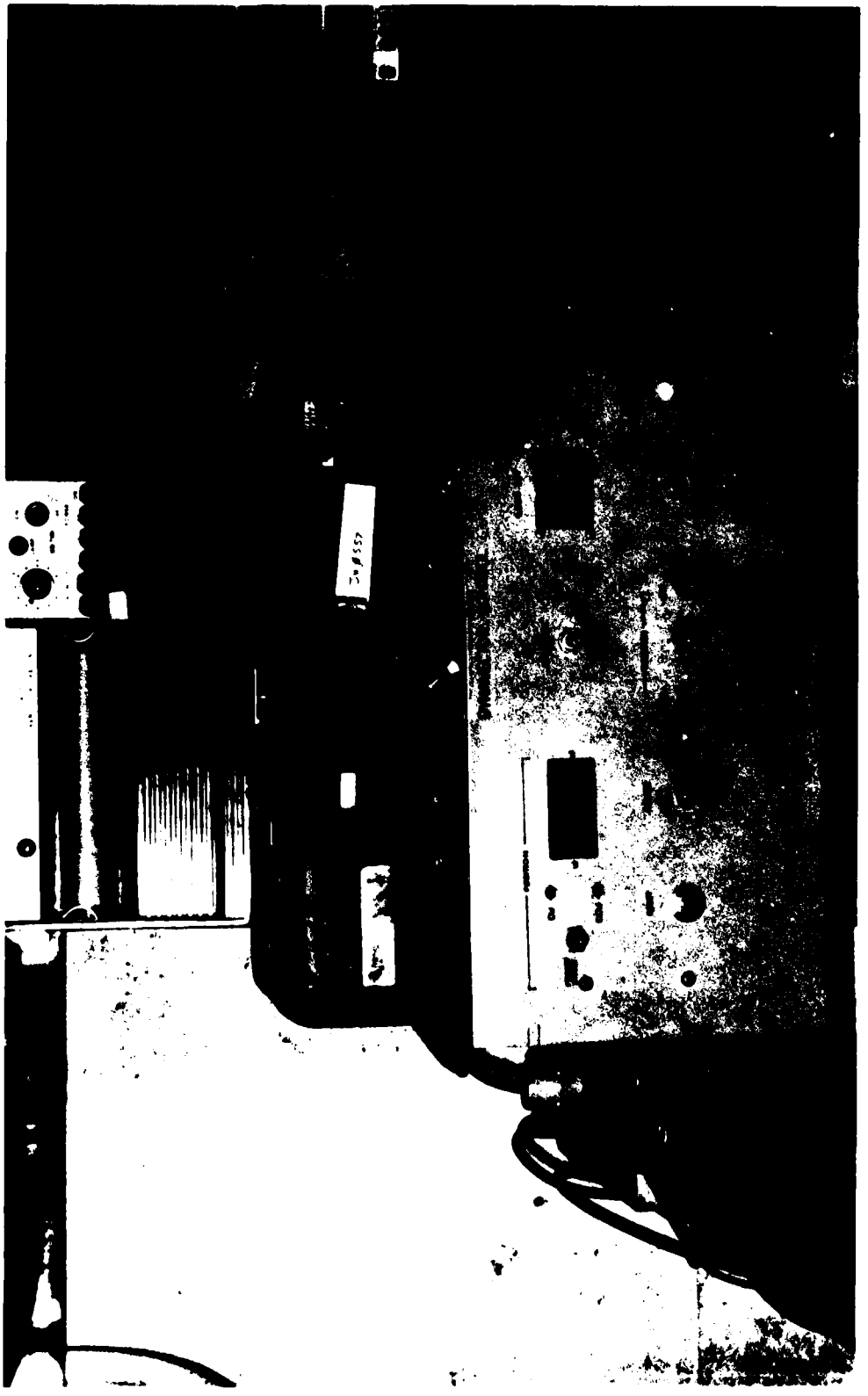

Figure 5. Actuator Control Chassis

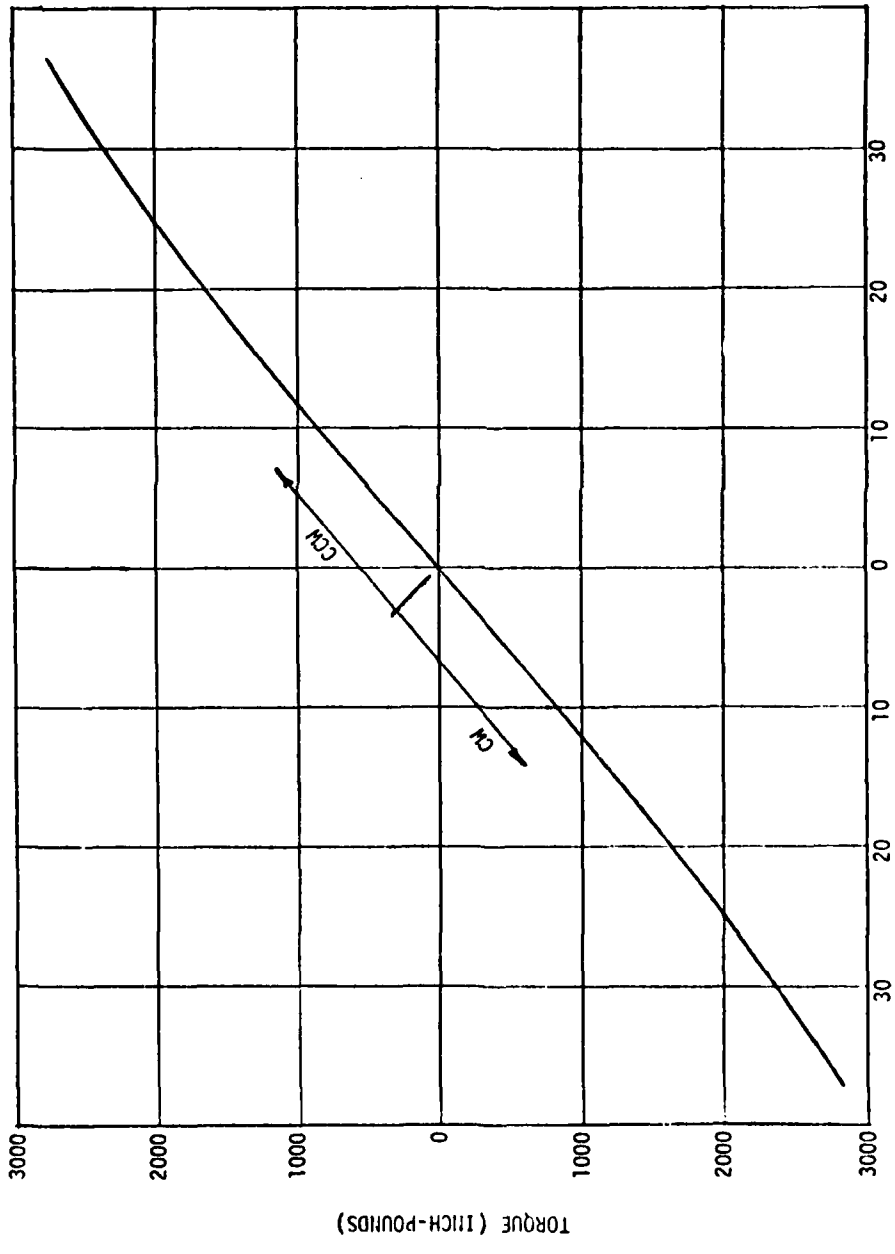

Figure 6. Dynavector Test Adapter Static Calibration

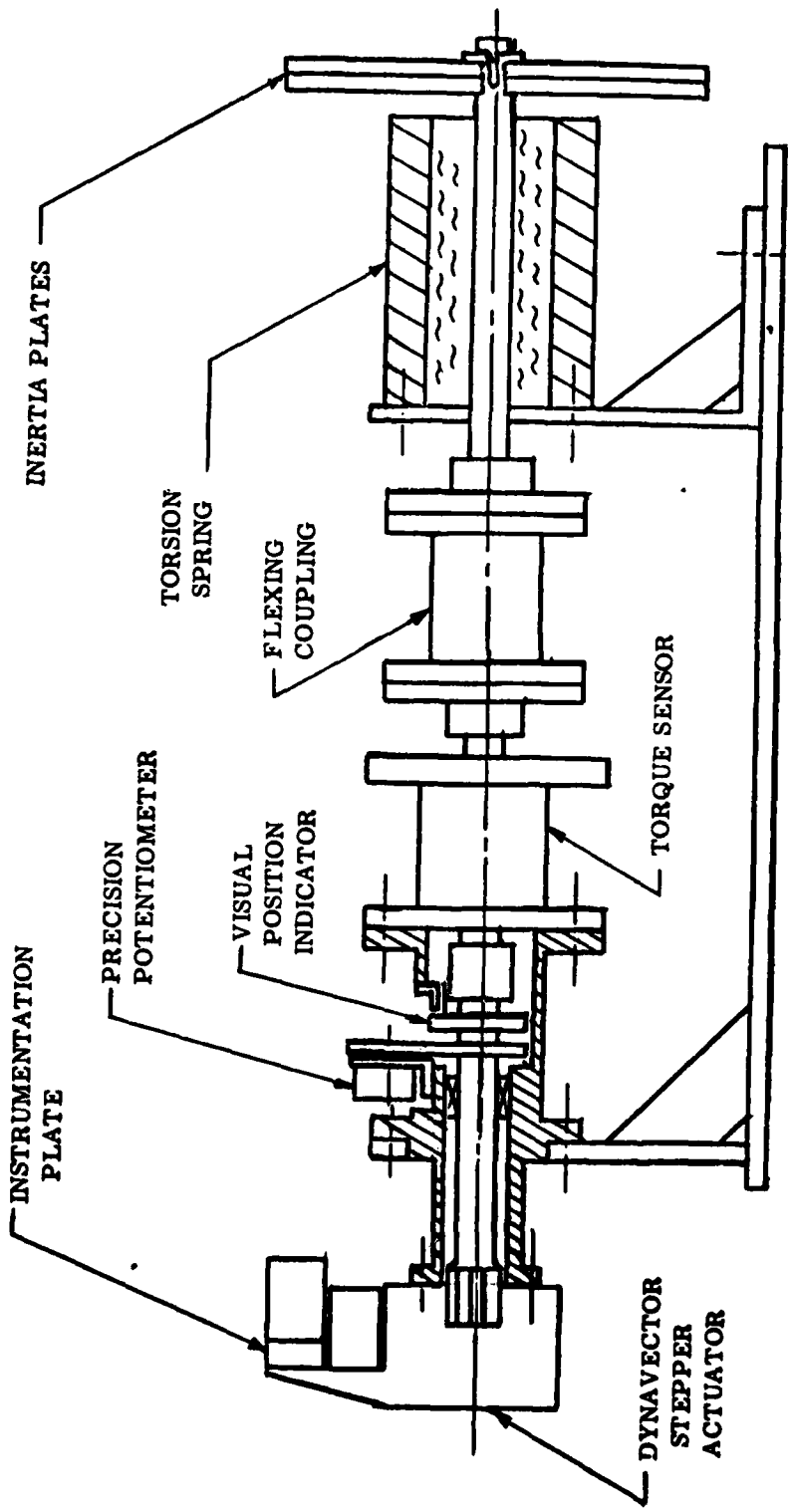

Figure 7. Actuator Test Stand

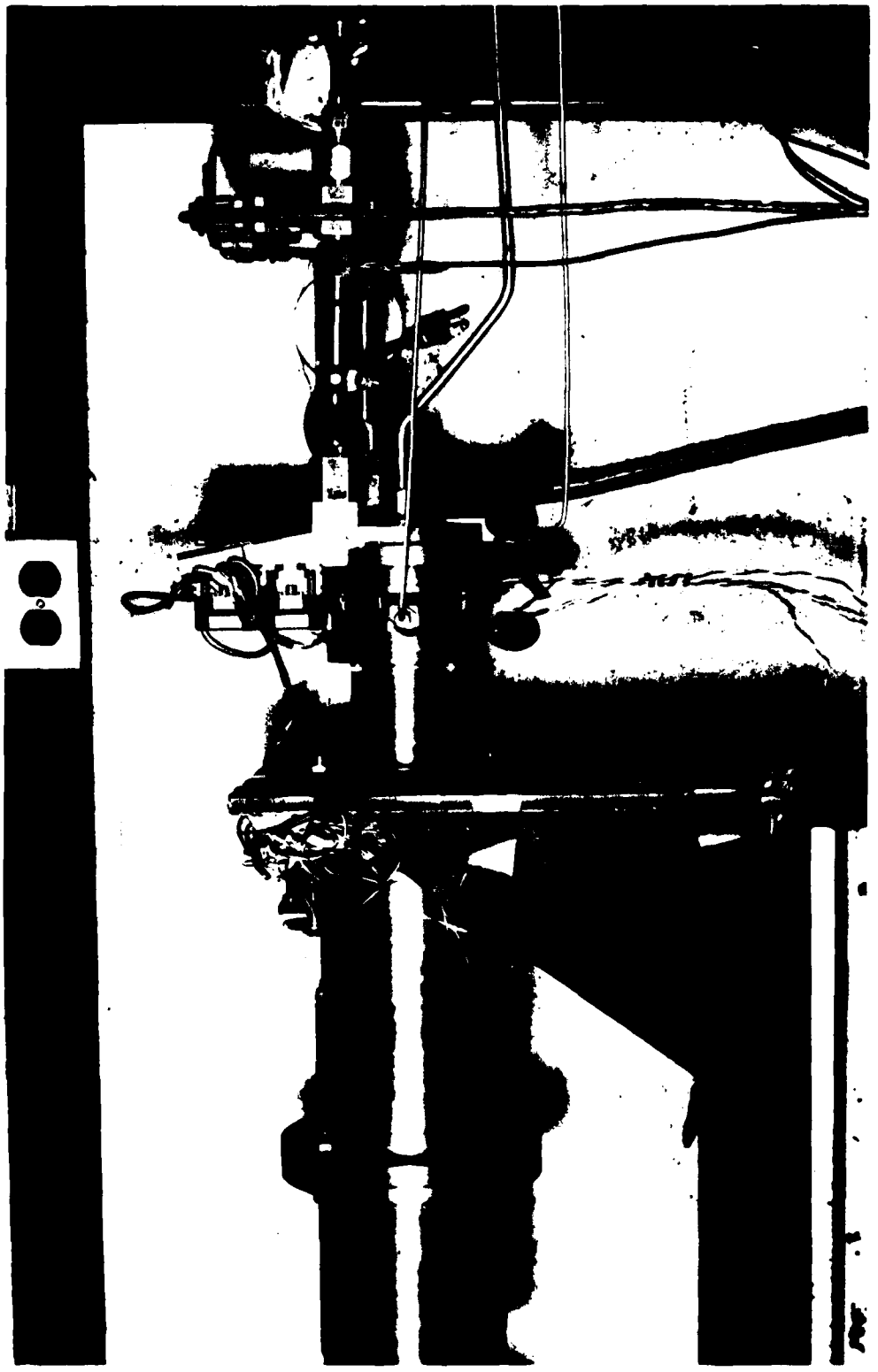

Figure 8. Actuator Assembled on Test Stand

Four Switching Valves are used to control the pressure of the eight motor chambers. Each valve controls two diametrically opposed chambers. One chamber will be at the supply pressure (3000 psi rated) and the other chamber at return pressure. When a valve is switched, the chamber pressures are reversed.

A modified Moog Type 30 servovalve was selected for this application. The Type 30 is a small (approximately 1.5 inch cube) 2-stage, 4-way flow control valve that is used extensively in aerospace applications. The feedback wire that normally connects the flapper to the second stage spool was removed (Figure 9) because proportionality is not required. The valves, modified with a high temperature coil, are rated at -65°F to +300°F with a 15-minute capability to 600°F.

The valves were supplied with three sets of spool end plates so that the effect of valve capacity could be evaluated. Evaluation was performed by Bendix Corporation. The end plates limit the spool travel and, therefore, the maximum flow rate. With the 100% stops, the maximum flow rate is 8 cubic inches per second. The other stops limit the flow rate to 75% (6 in^3/second), and 50 percent (4 in^3/second) of maximum flow. Testing proved that the 50% flow capacity gave optimum performance.

Instruments used included an oscillograph and a flow chart. The data that was recorded is as follows: flow (inlet and outlet), torque, and position. The examples of oscillograph recordings are labeled accordingly. The additional data that was hand recorded is frequency, mode, steps, and flow run time. Calibration on all instruments was checked periodically throughout the test.

SECTION III

TEST PROCEDURES

The type of tests performed were: static leakage test, stall torque, and life test.

1. STATIC LEAKAGE

Static actuator leakage data was taken for each of the 8 chambers at 3000 psi supply pressure. This data is displayed in Figure 12.

2. STALL TORQUE

Supply pressure for actuator is set at predetermined test pressure. The actuator is then stepped against the torsion spring until a stall condition is encountered. The stall condition is when the actuator fails to move against the applied torque. This procedure was performed for supply pressures of 1000, 1500, 3000 psi. Stall torque efficiency may be calculated from:

$$\eta_t = \frac{T}{b\ D_v\ \Delta P\ \ e\ \ R_t\ \sin\ \phi_\rho}$$

where

b, motor length = 0.439 inch

T, output torque = 2500 inch pounds

D_v, vane seal diameter = 2.9375 inch

P, pressure difference = 3000 psi

e, eccentricity = 0.0234 inch

R_t, gear ratio = 45:1

p, angle of pressure vector with axis of eccentricity = 90 degrees

$$\eta_t = \frac{2500}{0.439 \times 2.9375 \times 3000 \times 0.0234 \times 45 \sin 90} = 61.3\%$$

3. LIFE TEST

To perform the life test, the actuator was cycled ±20 degrees around zero at a rate of 140 degree/sec with a supply pressure of 3000 psi. The maximum torque incurred is ±1350 inch pound at ±20 degrees. Hand recordings were taken periodically throughout the test. The magnetic plug installed in the return line was inspected for particles every hour. Due to previous life test failures (1st 24 hrs., 2nd 34 hrs.) the actuator was disassembled and inspected after 20 hrs. of operation. After the inspection, the actuator was reassembled and testing was continued until the 50-hour requirement was met.

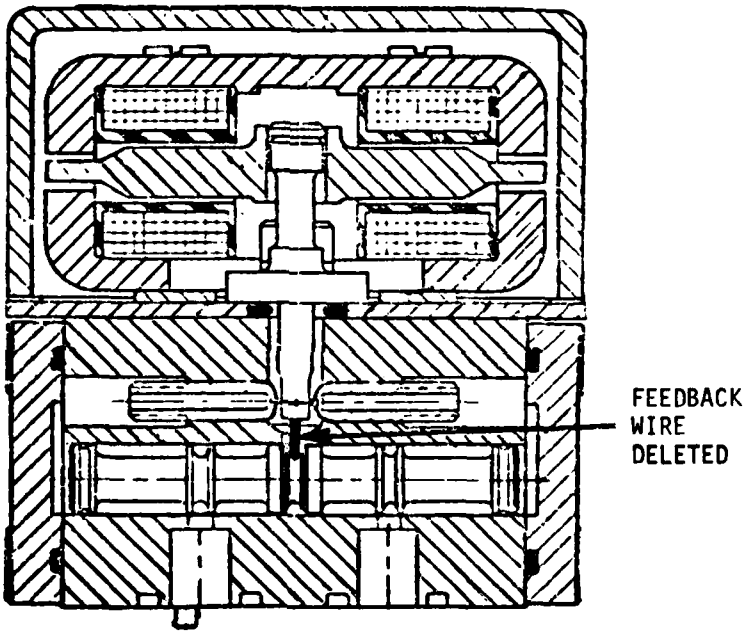

Figure 9. Moog Valve

TABLE 2

ACTUATOR CHARACTERISTICS

	Design	Demonstrated by Bendix
Hinge Moment (stall) (rated)	2000 inch-pounds 1333 inch-pounds	2400 inch-pounds 1330 inch-pounds
Vane deflection (maximum)	±35°	±35°
Vane rate (unloaded) (rated)	250°/sec (max) 140°/sec	670°/sec 390°/sec
Fluid	Chevron M-2V or equivalent	MIL-H-5606
Fluid pressure - inlet - outlet	3400 psia 400 psia	3000 psid pressure differential
Operating temperature - fluid	-65 to +600°F -65 to +550°F	No tests conducted except room temperature

SECTION IV

SUMMARY OF PAST RESULTS

The following tests were performed by Bendix Corporation at their research laboratory and previously reported in Reference 1. Results of static leakage test conducted by Bendix are shown in Figure 10.

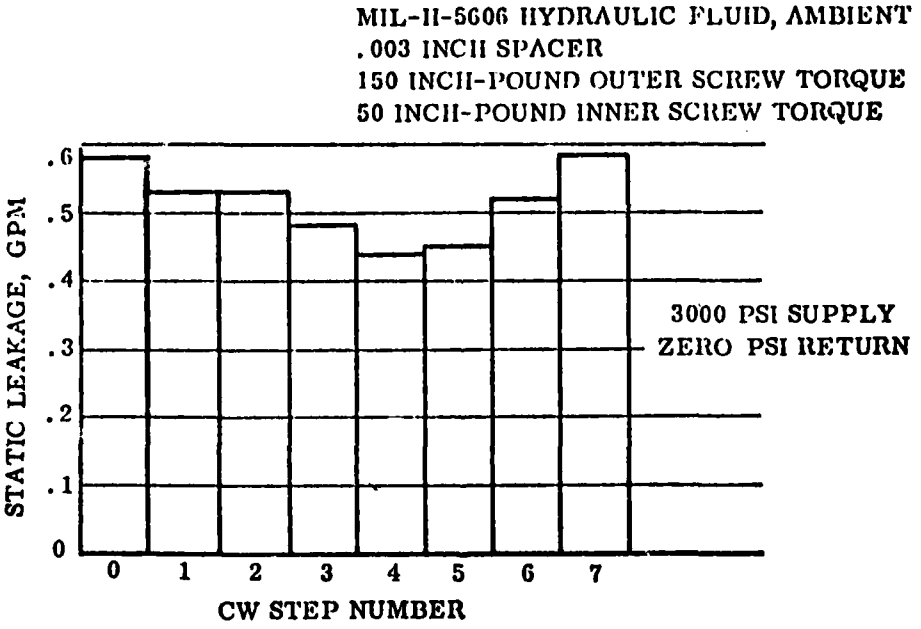

Figure 10. Static Leakage Test Results from Previous Bendix Program

Results of Bendix's stall torque test are shown in Figure 11.

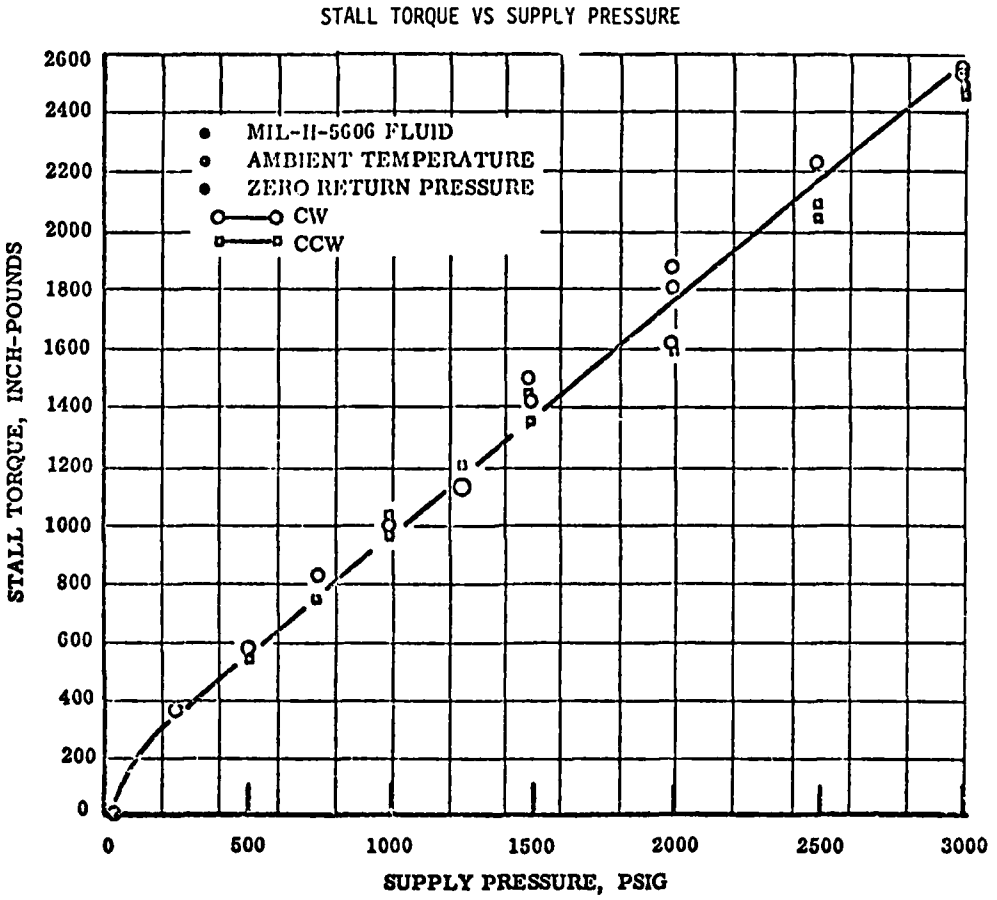

Figure 11. Stepper Actuator Break-In Stall Torque from Previous Bendix Program

BENDIX LIFE TESTS RESULTS

Results of the first life test were unsatisfactory. During the first life test, the actuator began to lose steps and cycle erratically. The test was stopped and the magnetic plug was inspected. It was covered with many particles. The life test had been run for 23.7 hours. The

actuator was disassembled and inspected. Two of the reaction pin spacers were missing. The others showed severe deterioration. The rotor was badly scored in spacer holes and adjacent areas. The rest of the actuator appeared to be in normal condition.

It was concluded that the fatigue failure was due to decarburization of the reaction pin spacers. New pins were fabricated taking special precautions to prevent decarburization. The actuator was then reassembled using new seals, bearings, screws, rotor, and shaft. Break-in tests were run. The performance was essentially the same as the original.

Procedure for the second life test was the same as the first. The life test proceeded well for 34 hours, then was stopped when a large (0.06 x 0.09 x 0.0025 inch) chip was found in the return line. No deterioration in performance had been detected. Total time on the actuator was 39.2 hours. The actuator was disassembled and inspected. The number 4 spacer was fractured into several pieces. Under magnification, other spacers showed signs of deterioration (cracks).

Analysis of the failure resulted in a recommendation to change the reaction pin spacer material from M-2 tool steel to VASCO wear tool steel. Vasco tool steel has nearly equivalent compressive strength and wear characteristics but is appreciably tougher. The actuator was rebuilt with Vasco wear tool steel reaction pin spacers and then delivered to the Aero Propulsion Laboratory for performance testing. The results of this performance testing is contained in Section V.

SECTION V

AFAPL TEST RESULTS

The following are the results of testing at AFWAL on the actuator rebuilt by Bendix:

1. STATIC LEAKAGE

Static leakage data was taken at a supply pressure of 3000 psi using Mil-5606 hydraulic fluid at ≃80°F. This test was performed before and after the life test. The results indicated virtually no change in static leakage performance. Data is shown in Figure 12.

2. STALL TORQUE

Stall torque test was performed before life test, after teardown (teardown occurred at the 20th hour of life test), and after the life test. The results are shown in Figures 13, 14, and 15.

3. LIFE TEST

The life test proceeded with no actuator mechanical difficulty, although some other problems were encountered. A summary of test conditions and results are shown in Table 3. Just after 6 hours of testing, a fluid supply hose ruptured. It was replaced and testing was resumed. After 11 hours, the actuator began to bypass the limit of 20 degrees and drive to the stall condition before switching directions. This happened several times and appeared to be an electrical problem. The problem was corrected and the test proceeded. At the end of 20 hours, the actuator was disassembled and inspected. No sign of deterioration was found so the test was continued. After several hours, the return line filter element was removed and cleaned. No metal was found, but a large amount of fine rubber particles were removed. The rubber particles were introduced into the system when the high-pressure hose burst. The test was resumed (using the same filter element). The test was completed with no sign of actuator failure.

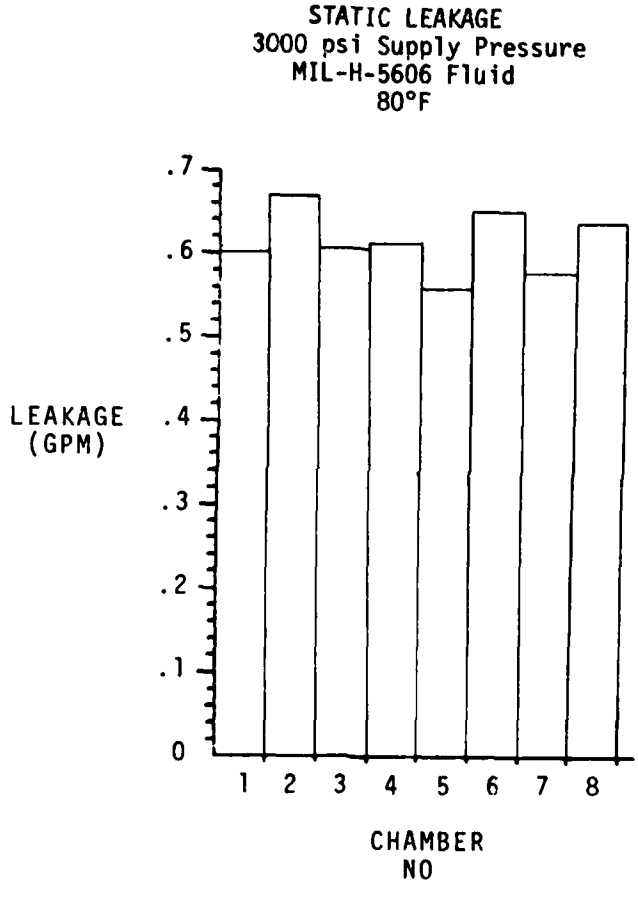

Figure 12. Static Leakage of Actuator

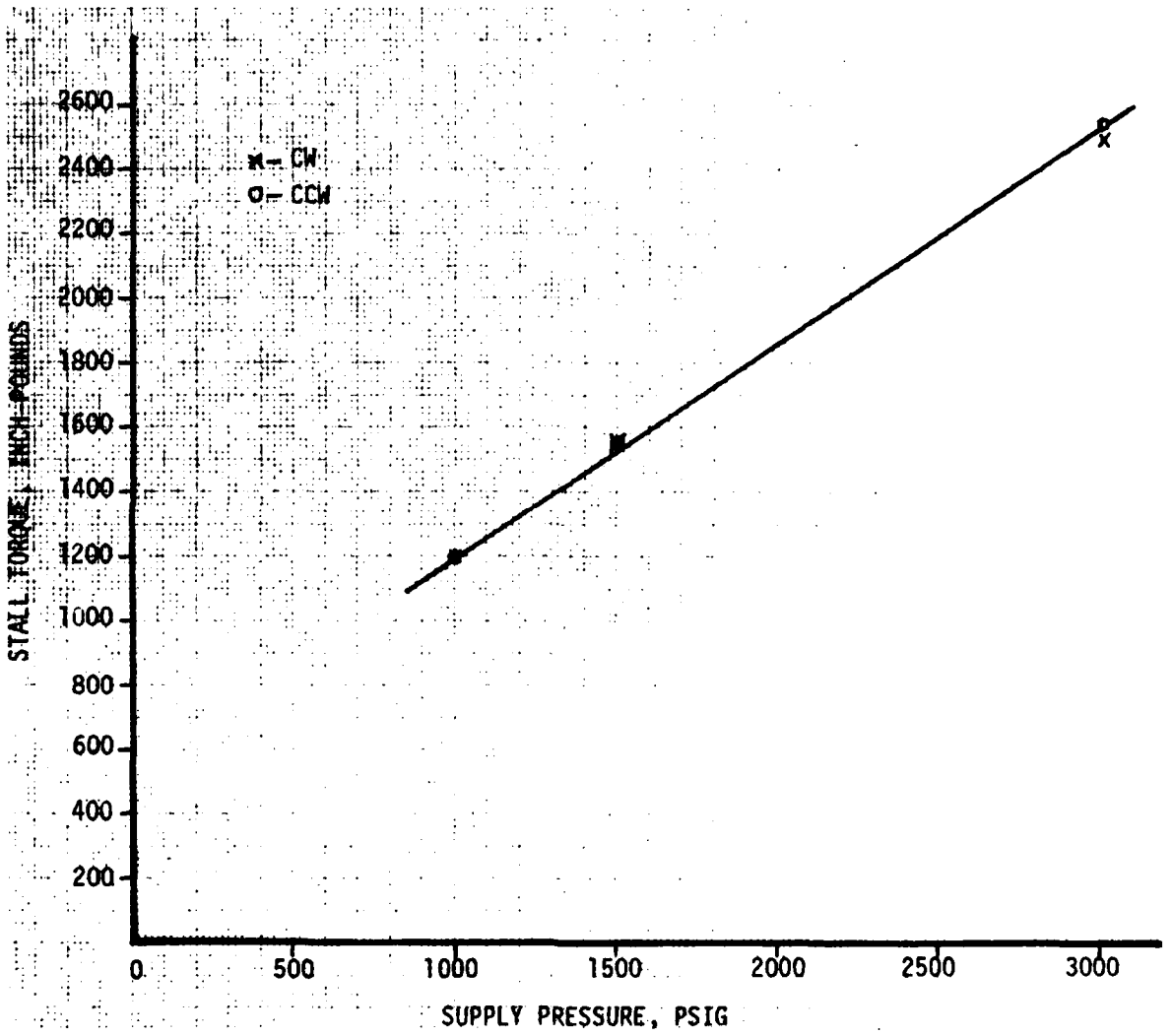

Figure 13. Stall Torque Test Data Performed Before Start of Life Test

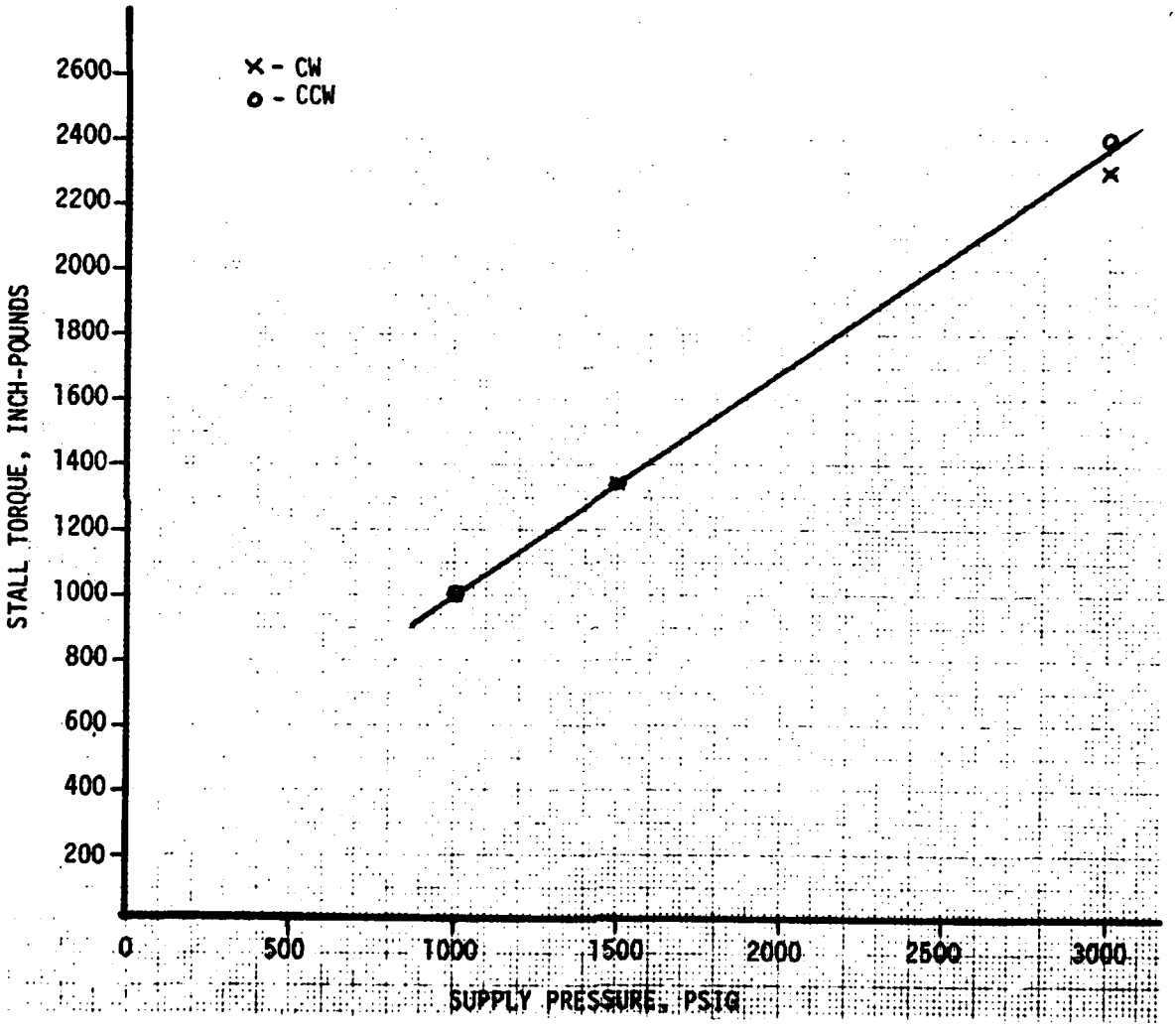

Figure 14. Stall Torque Test Data Performed After 20 Hours of Life Test

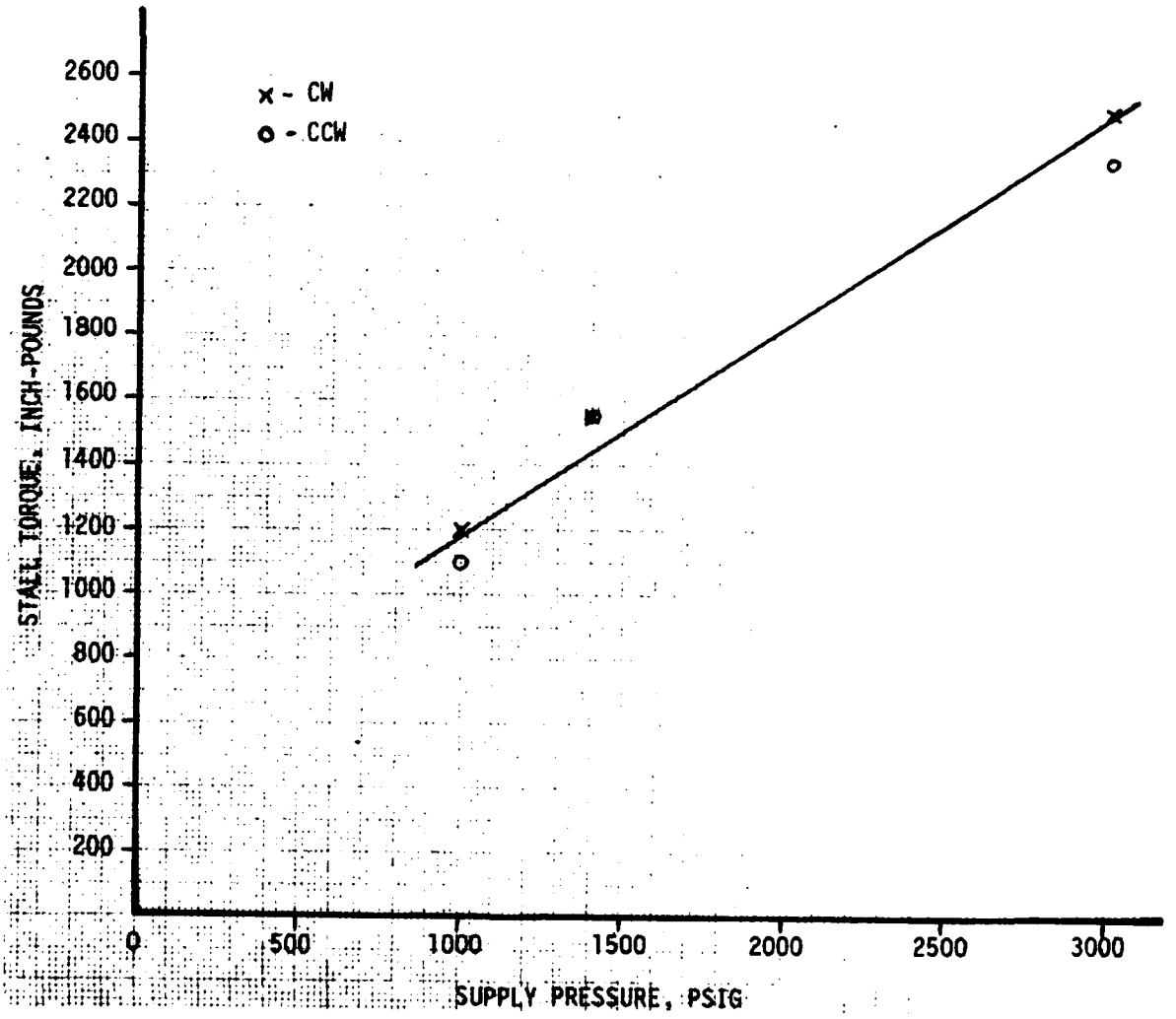

Figure 15. Stall Torque Test Data Performed After Completion of Life Test

TABLE 3

SUMMARY OF LIFE TEST

Hours	- 50
Cycle Rate	- 140 degree/sec
No. of steps	- 25,200,000 steps
Average flow	- 3.35 gpm
Dynamic flow	- 2.65 gpm

SECTION VI

CONCLUSIONS AND RECOMMENDATIONS

CONCLUSIONS

1. The actuator met all the design requirements. The reaction pin spacer problem appears to be solvable but has reduced the overall success of this program.

2. The repeatability and accuracy of the actuator, without feedback, is very impressive. The use of direct digital input without feedback for advance missiles appears very attractive for application where digital computers are being used for guidance and control. Also, the capability of this approach for high temperature applications, where null shift is a problem with conventional electrohydraulic servo's, appears to be very attractive.

RECOMMENDATIONS

1. The following are recommended approaches to solve the reaction pin spacer problem:

a. After heat treatment, the outside diameter and inside diameter of the spacer should be jig ground to a fine microfinish. The spacer housing should also be ground or lapped to ensure a smooth contact surface between spacer and housing. The lapped contact surface should greatly reduce fatigue caused by abrasive wear.

b. Additional flow should be supplied into the spacer area. The leakage would lubricate and clean the contact surfaces. Again this would reduce fatigue from abrasion (scoring, fretting, etc.).

c. Enlarge the outside diameter of the reaction pin spacer. This would decrease the overstress problem encountered with the spacer size being used.

2. The testing to date has proven the feasibility of this approach. Further testing of this actuator is not recommended because of the reaction pin problem.

Every hour throughout the test, the magnetic plug in the return line was inspected. Several times (occurring randomly) the plug had a small amount of very fine metal particles on it. The actuator's performance did not change at these times nor at any other time throughout the test.

At the end of the life test, the actuator was disassembled and inspected. The number one reaction pin spacer, shown in Figures 16 and 17, was broken into four pieces. Reaction pins are shown in Figures 18 and 19. The other reaction pins and other parts of the actuator, as shown in Figures 20 through 23, appeared to be in good condition. The pieces of the broken pin all had sharp edges and showed no sign of being crushed. The magnetic plug was clean after the 50th hour.

The mechanical portion of the actuator performed satisfactorily throughout the 50-hour test except for the reaction pin spacer failure. The fact that the pin had not been crushed seems to indicate that it had not been broken very long. The reaction pin spacer which failed was sent, along with two other spacers and three reaction pins, to the Bendix Research Laboratory (BRL) for analysis. At BRL the pieces underwent microscopic examination, hardness measurements, and EDAX analysis procedures. The complete BRL report is contained in the appendix of this report.

The following is an outline of some of the more critical findings from BRL. The outer surface of the failed spacer contained a large number of deep long cracks. These cracks originated at the outer surface and propagated inward, thus, causing the spacer to fail. The cracks found on the failed spacer indicate that the spacer was overstressed. Poor finish machining is the apparent cause of the abrasive wear (scoring and spalling) on the failed spacer.

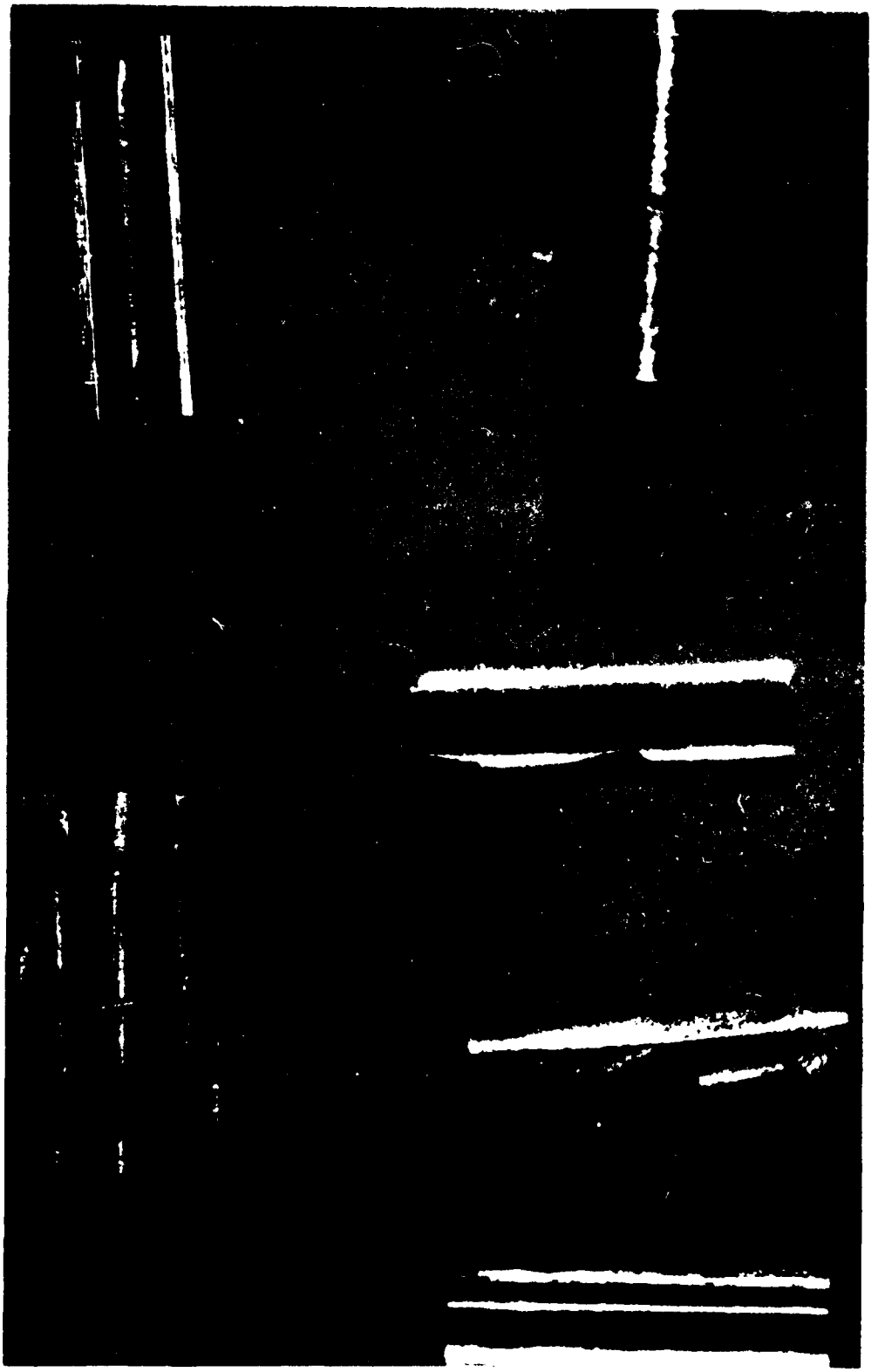

Figure 16. Failed Reaction Pin Spacer

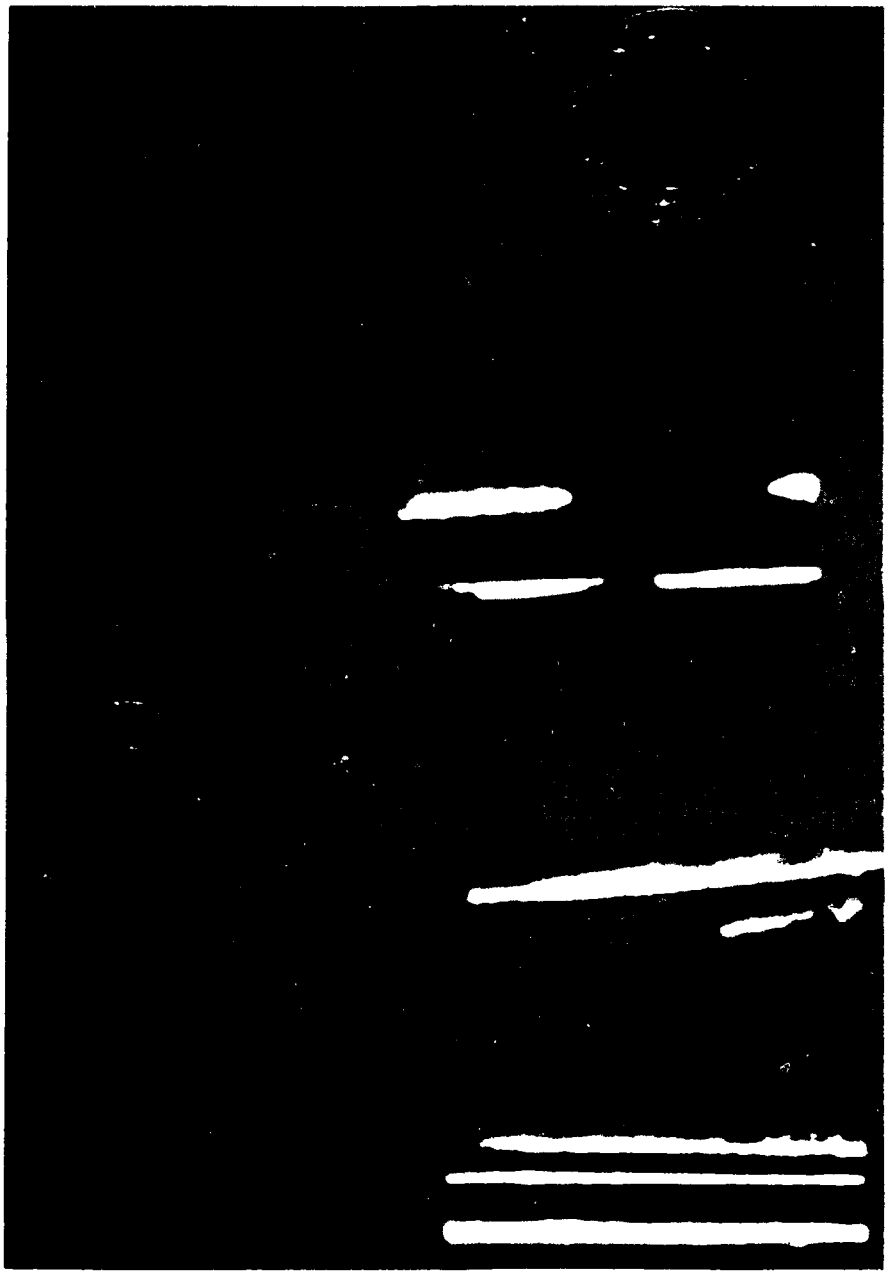

Figure 17. Failed Spacer, A Vane, and A Nonfailed Spacer

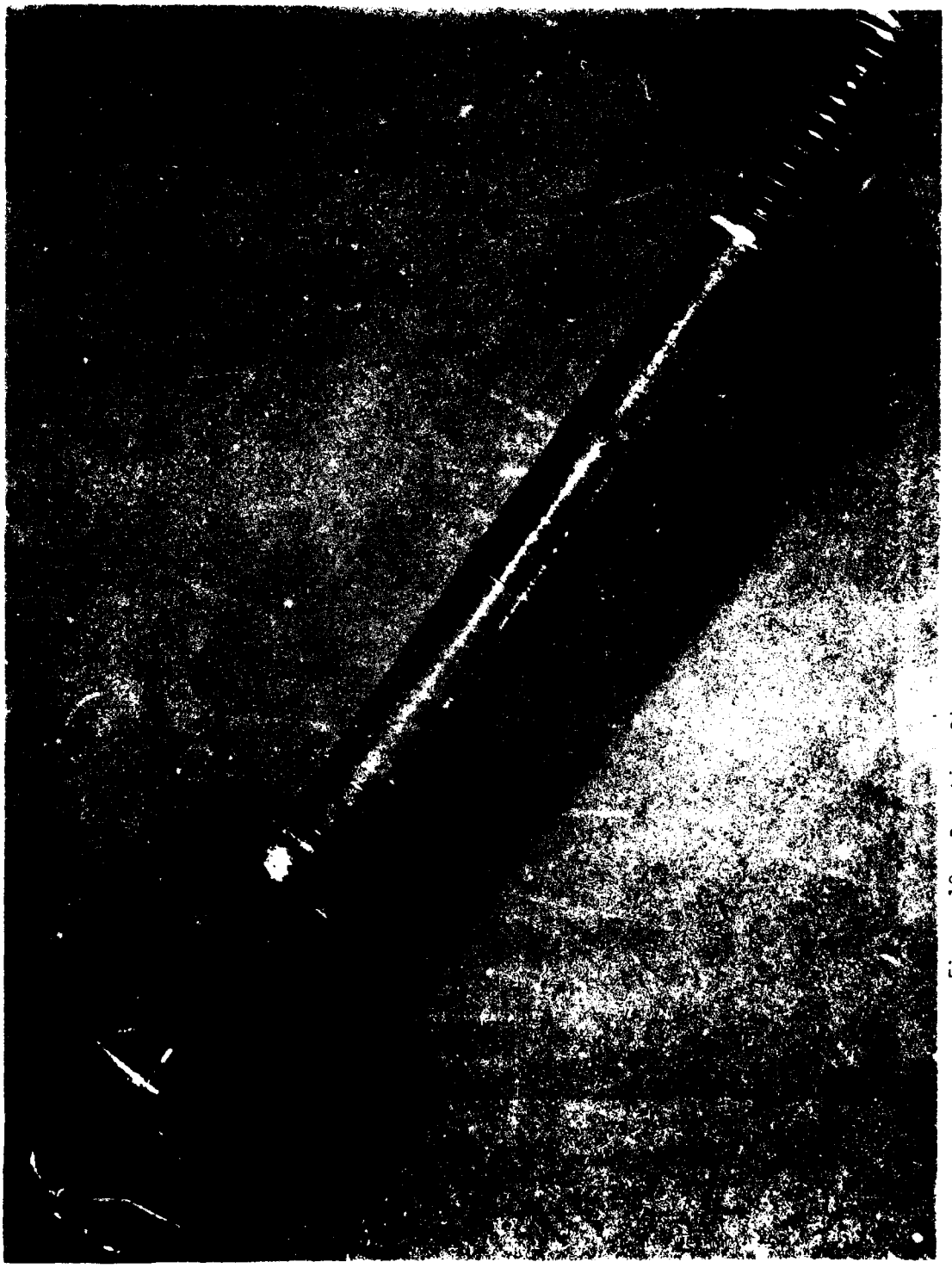

Figure 18. Reaction Pin
(After 50-Hour Life Test, Taken from a
Nonfailed Spacer)

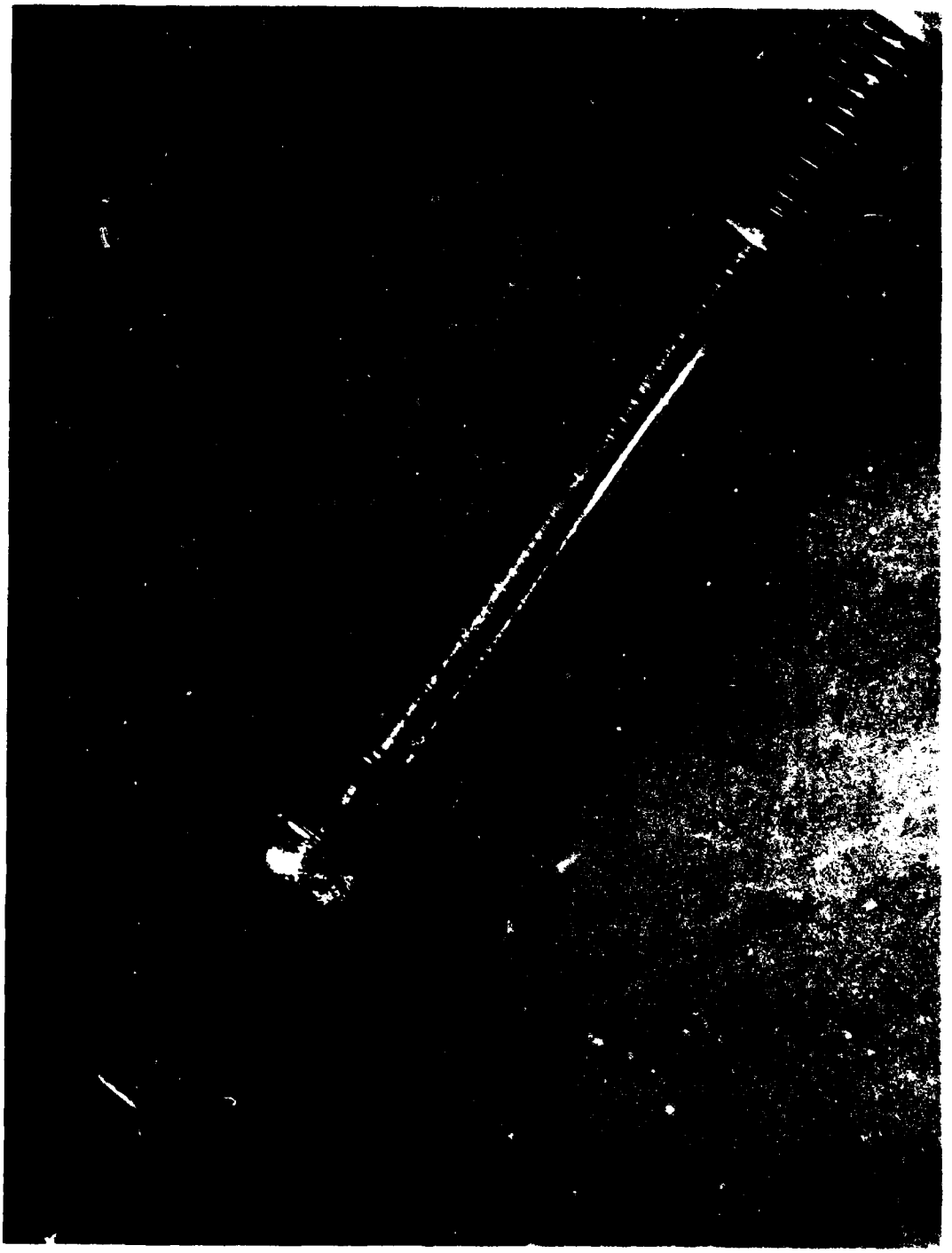

Figure 19. Reaction Pin
(From a Failed Spacer After 50-Hour Life Test)

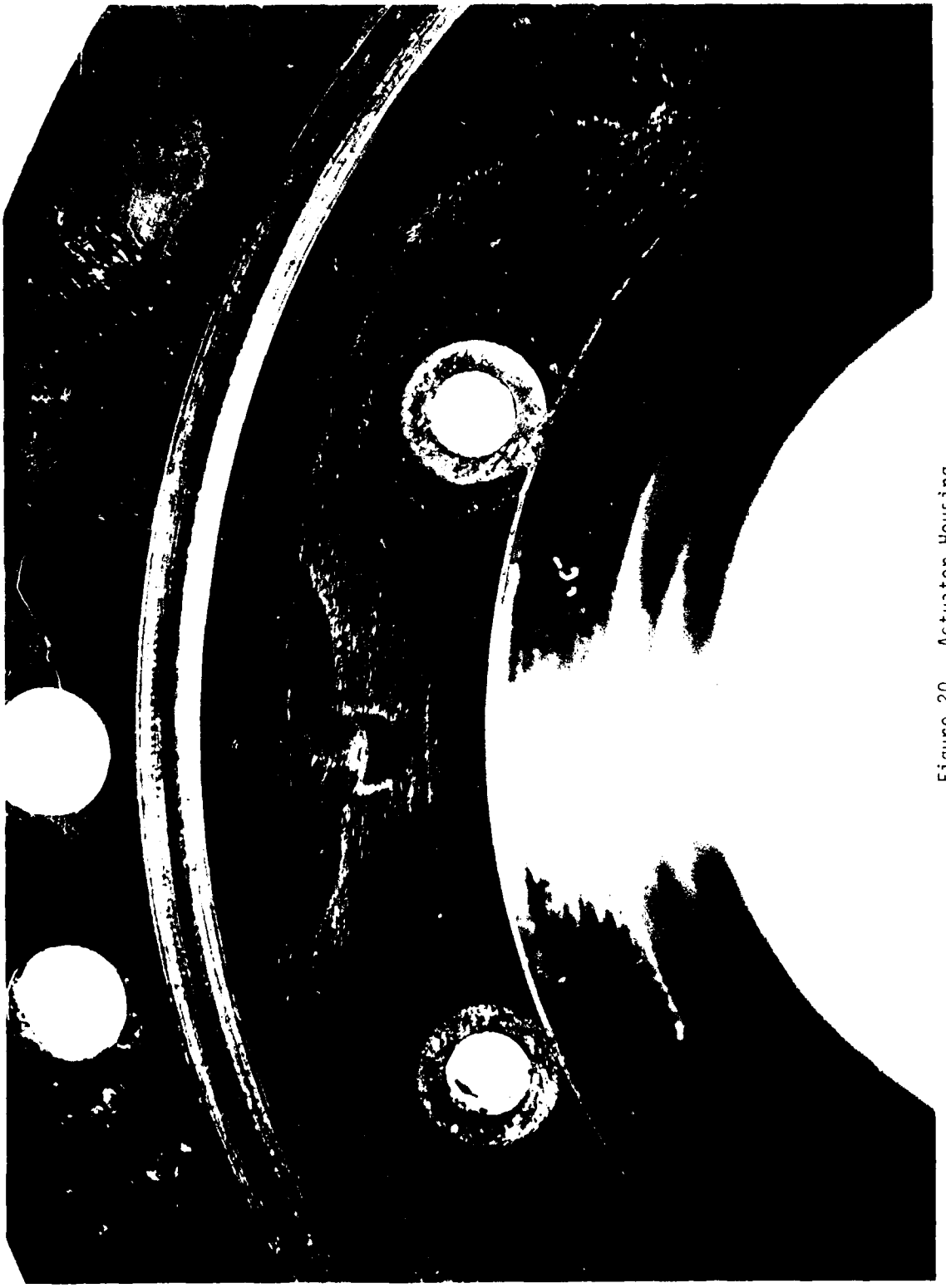

Figure 20. Actuator Housing

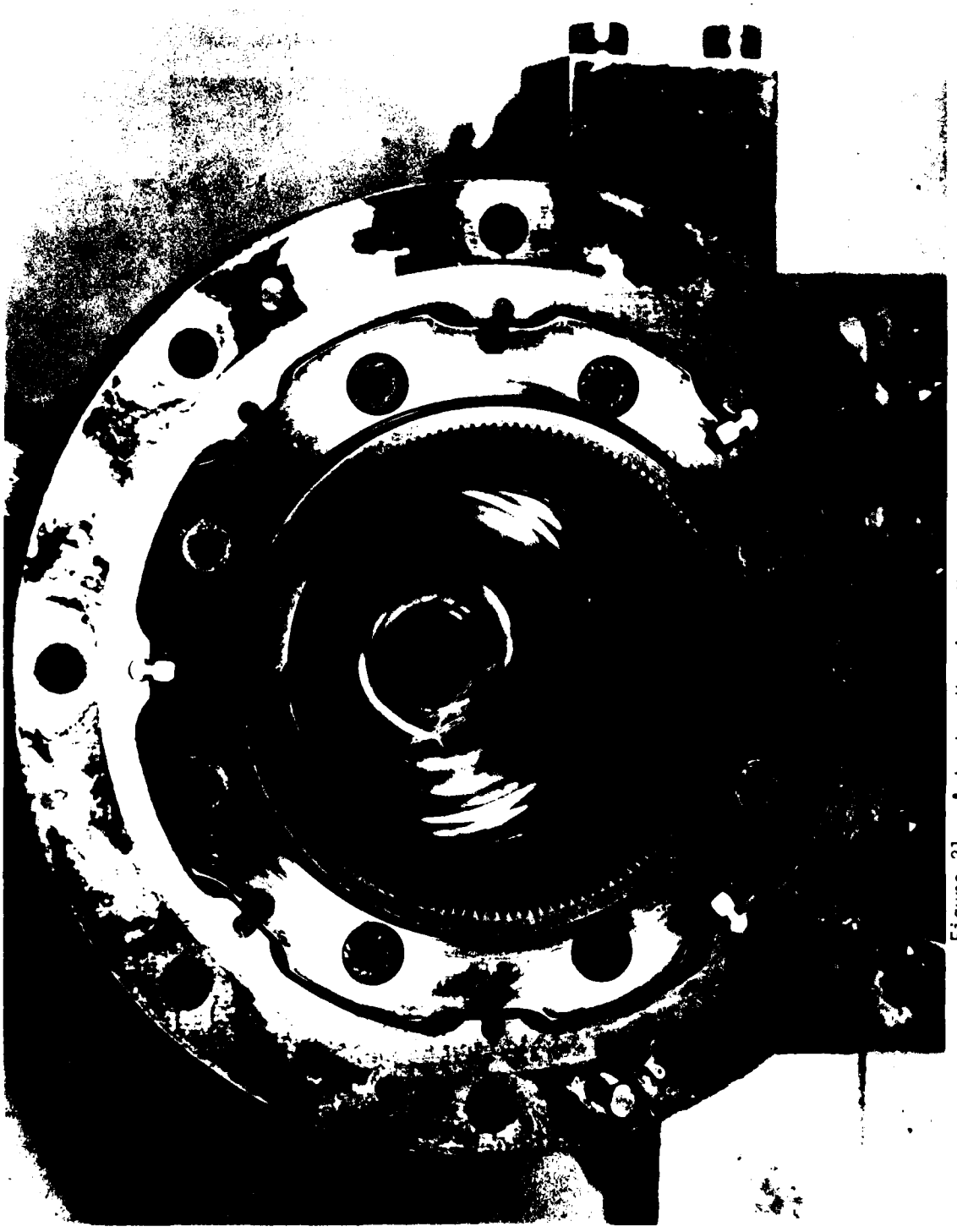

Figure 21. Actuator Housing, Vanes, Spacers, and Rotary Motor Before Disassembly

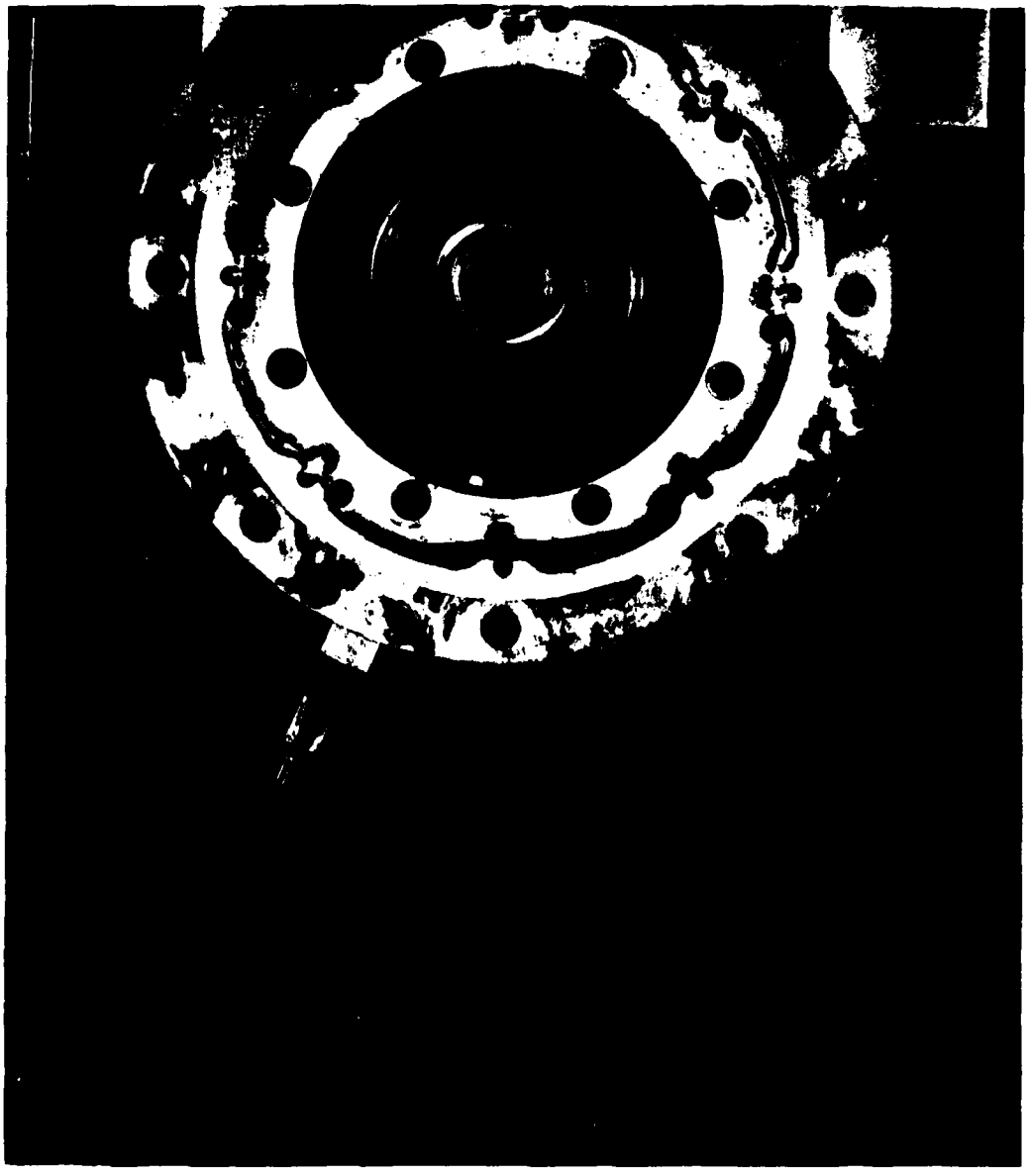

Figure 22. Actuator, Spacers, and Vanes

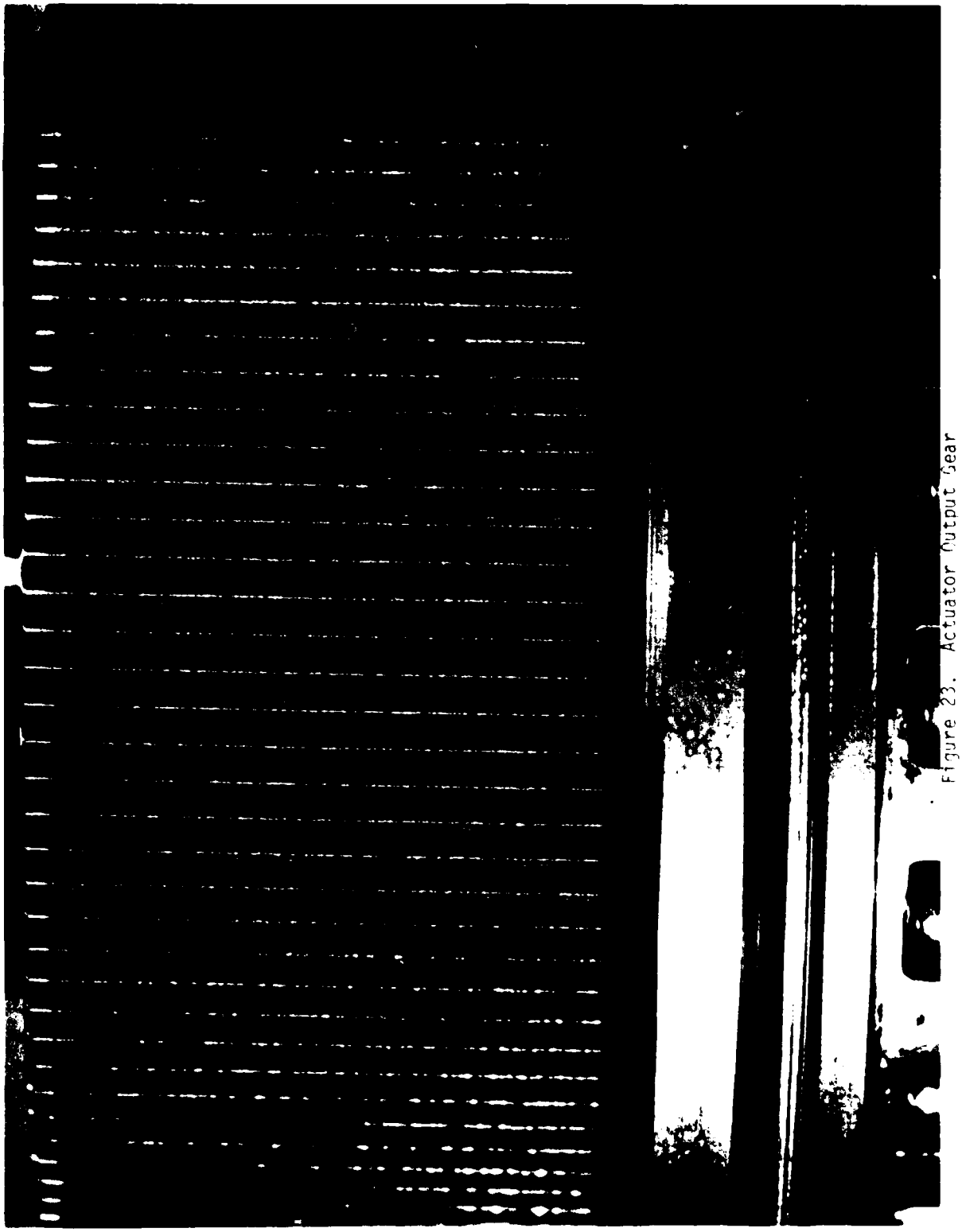

Figure 23. Actuator Output Gear

REFERENCES

1. Jack M. Silvius, Digital Electrohydraulic Stepper Actuator for Advanced Missile Systems, Bendix Corporation Aerospace Systems Division, Mishawaka, Indiana 46544, June 1978.

2. K. E. Amin, Failure of Reaction Pin Spacer on Model HL-045-U1 Dynavector Actuator, Bendix Research Laboratories Internal Memorandum, Appendix of this report.

APPENDIX

BENDIX RESEARCH LABORATORY
REPORT OF REACTION PIN SPACER
FAILURE

Internal Memorandum

Bendix Research Laboratories

Date May 7, 1979 Letter No. Southfield, Michigan

To J. M Silvius, Bendix Aerospace System Division/Mishawaka Operations

From K. E. Amin

Subject Failure of Reaction Pin Spacer on Model HL-045-U1 Dynavector Actuator

---

A reaction pin spacer, which failed during the 50 hour life test of the Dynavector Actuator at WPAFB, was sent to BRL along with two other spacers and three reaction pins that experienced the same test for identification of the most probable cause of failure.

A previous study[1] of spacer failure (at BRL) attributed that failure to strength reduction by decarburization of the spacer during heat treatment. Care was then taken to avoid decarburization; however spacer failure was again experienced and new BRL studies[2] determined that failure at that time was a result of cracking (surface damage) of spacer bore by abusive grinding (or honing) during the final machining operation. Replacement of the spacer material (M2 tool steel) by a tougher alloy (cold worked die steel) was then recommended and implemented. However one of the reaction pin spacers failed, and the following investigation was initiated to look into the problem once more. Microscopic (optical and scanning) examination, hardness measurements and EDAX were carried out on the provided pieces and the following is a summary of observations:

The outer surface of the spacer which failed during the life test contains a large number of deep long cracks, originating on the surface and running parrallel to the spacer axis. Evidence of abrasive wear and some adhesive wear damage and poor surface finish (from machining) is observed, along with residue of debris particles and chips (Figures 2 to 6).

The failed spacer inner surface (bore) shows some surface damage in the form of scoring, spalling (microspalling) and pitting resulting from both abrasive wear (during testing) and poor machining (during fabrication). However, almost no cracks were found on that surface (Figure 7).

Both inner and outer surfaces of those spacers which passed the life test show little damage and cracking, some brinelling (surface indentations), and contain almost no trapped particle (or debris)(Figure 8 and 9).

Surface of the Dynavector pin, which was in contact with the failed spacer reveals slight abrasive damage (Figure 10). The pin has a 0.179 in diameter, slightly larger than the design requirement (0.165 to 0.175 in.).

Internal Memorandum

Bendix

Date May 7, 1979 Letter No.

- o Fracture surfaces reveal multiple crack initiation and propagation sites; initiation sites were on the outer surface and propagated by fatigue to a final brittle failure. Quasi-cleavage facets and deep cracks exist all over the fracture surface indicating still a lack of sufficient ductility combined with spacer overstressing.

- o EDAX analysis of the adhesive layer on the outer surface of the failed spacer shows almost no vanadium (Figure 6); the spacer material contains about 2.4% vanadium, while the rotor contains negligible amount of vanadium (< .6%).

- o Microstructure of all spacers (failed and not failed) is uniform and shows no evidence of either decarburization or microstructural defects (such as segregation, banding, etc.) (Figures 19 and 20).

- o Hardness measurements taken on different sections of both the failed and not-failed spacers yield values in the range of 49 to 56 Rc; this steel when air hardened should yield 60 Rc minimum.

Discussion and Conclusion:

From the evidence presented so far, it appears that fracture of the spacer occurred as a result of its outer surface damage, which provided multiple crack initiation sites and facilitated crack propagation, leading ultimately to premature failure during the life test. Damage of the spacer surface occured during a sequence of events starting during the lengthy machining and heat treatment steps (leaving scratches, scores, asperities, and high residual stress sites), and then during the life test essentially by abrasive wear, as well as by some adhesive wear, of any trapped particles during relative motion (sliding) of rotor and spacer (opening new cracks and enhancing propagation of existing cracks). Those trapped particles probably existed on the original surfaces (rotor and spacer) as a result of insufficient cleaning after various processing (machining and heat treatment) and/or formed by breaking either surface-asperities and debris formation (enhanced by rough surface finish, oxidation and differnece in relative hardness of the sliding surfaces) during the life test. It appears that the adhesive layer composition is closer to that of the rotar material. The inner surface of the rotor was not available for examination.

Internal Memorandum

Bendix

Date May 7, 1979 Letter No.

page 3

Recommendation:

1. The contacting surfaces (rotor and spacer) must be fabricated to a smooth surface finish, and thoroughly cleaned following the lengthy machining and heat treatment step, so as to minimize the presence of trapped particles and avoid surface damage by wear.

2. Again, final machining should be carried out gently and in no way should result in surface scoring, and damage, since fatigue life of the spacer is very sensitive to its surface condition.

3. During the heat treatment, triple tempering in air might be replaced by a double treatment in an inert atmosphere, and hardness values 60 Rc or higher should be achieved (this also provides the desired alloy high compressive strength).

Kamal E. Amin

KEA/pkf

cc: P. C. Becker
M. H Gardon
W. H. Gruber
L. L. Hartter
K. Lawson
L. F. Mayer
S. K. Rhee

Internal Memorandum

Bendix

Date May 7, 1979 Letter No.

References

1. J. H. Tarter, "Investigation of Failure of Reaction Pin Spacer on Model HL-045-U1 Dynavector Actuator," BLR/TM-77-8492 (August 1977)

2. S. Ganesh "Failure Analysis of Reaction Pin Spacer on Model HL-045-U1 Dynavector Actuator", BRL/TM-77-8514 (September 1977)

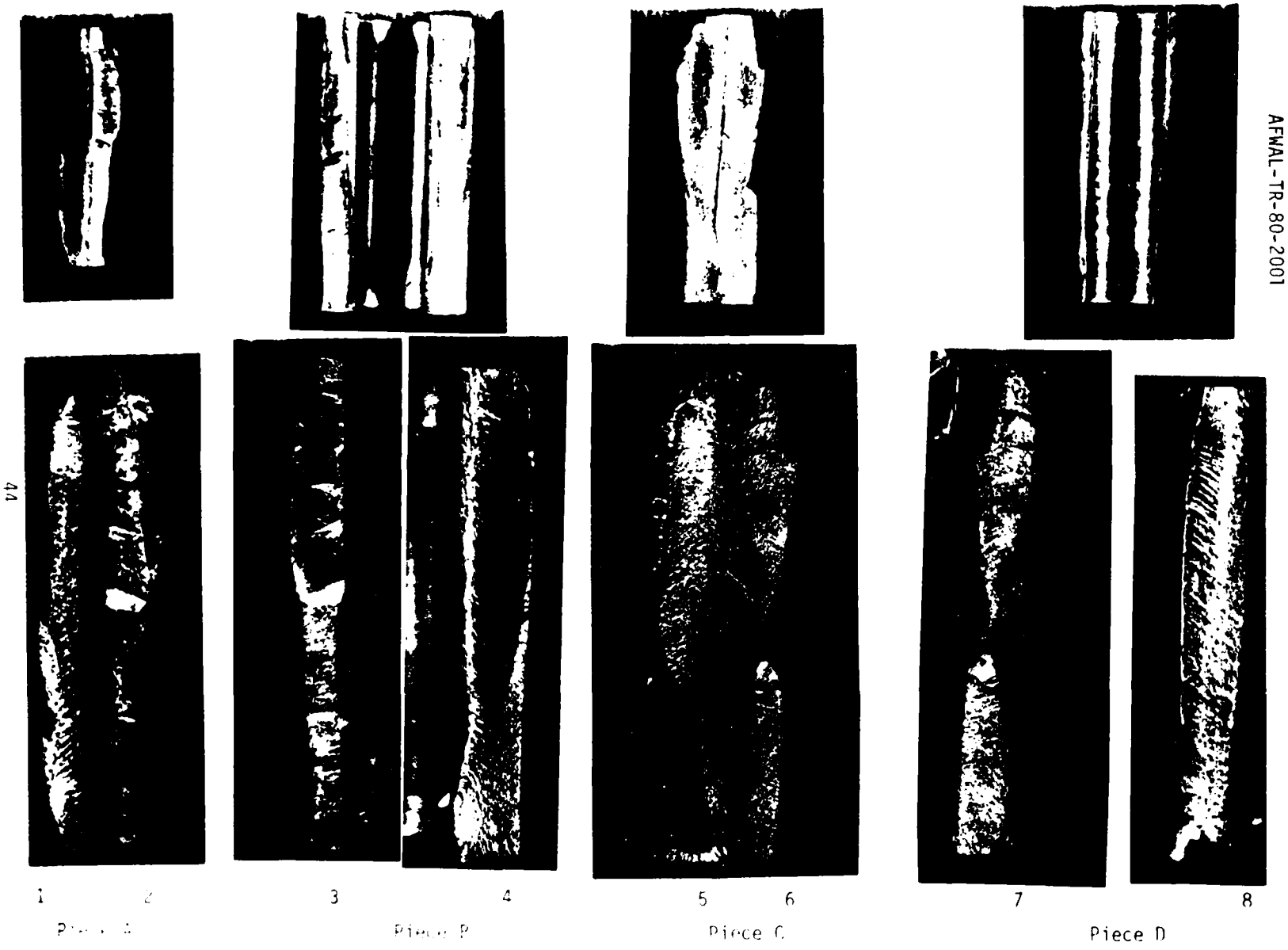

Figure 14. Parts of the Overspeed Actuator reaction pin spacer which failed during the 50 hour life test.

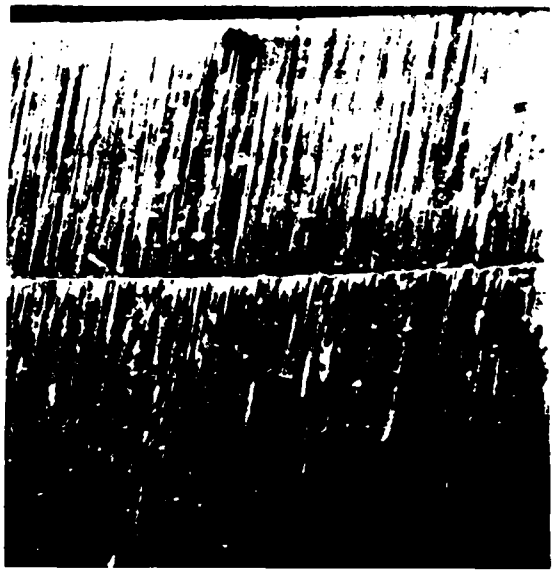

Crack area A above 100X

-Crack area B above 50

45

- Crack area C above 500

Figure 2. Outer surface of pin spacer piece A (of Fig. 1), showing the presence of deep long cracks running parrallel to the spacer length. Evidence of abrasive wear and poor initial surface finsih (machining) is observed, along with the presence of debris and chips.

Figure 3. Outer surface of Pin spacer piece B, showing abraded surface full of scratches, surface pits, and many cracks originating from the spacer outer surface.

20X

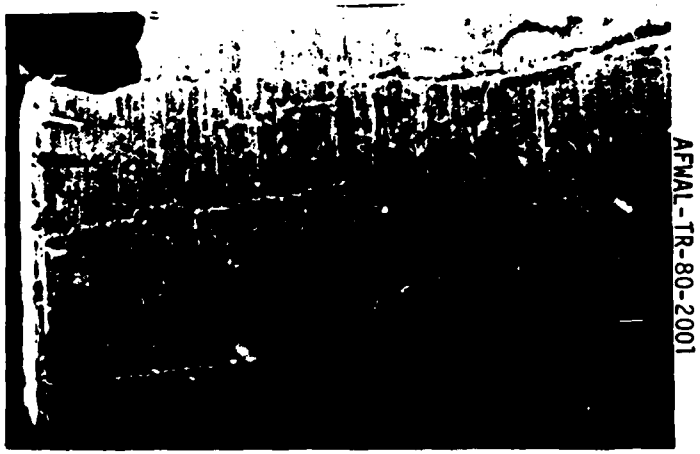

50X

A 500X

B 500X

Figure 4. Outer surface of piece C showing the same surface damage observed for pieces A and B, and the presence of particle chips. Notice the deep grooves and scratches (impressions) caused by those particles sliding against the spacer surface.

a - 20X

b- Area near 3 (left). 200X

Figure 5. Outer surface of piece D, showing evidence of adhesive wear (microspalling), (A), as well as abrasive wear (B,C,D,etc).

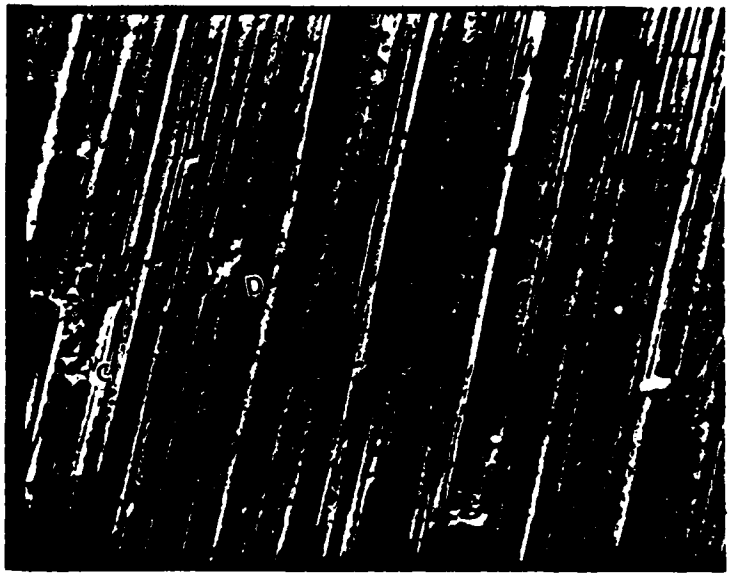

c - area 4 above enlarged 500X

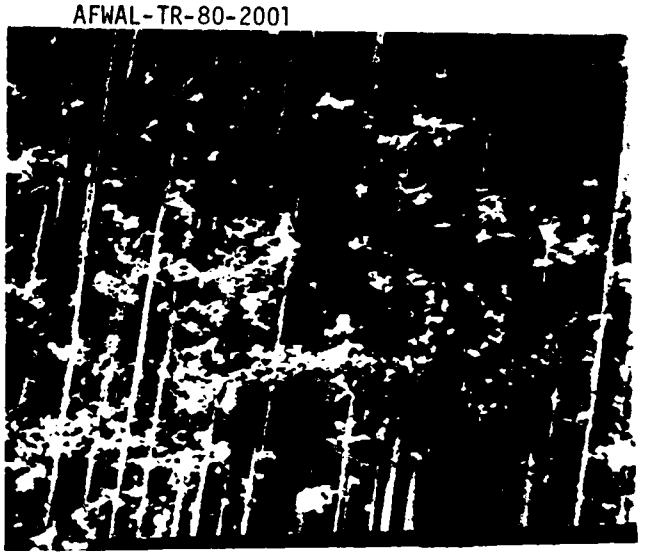

500X

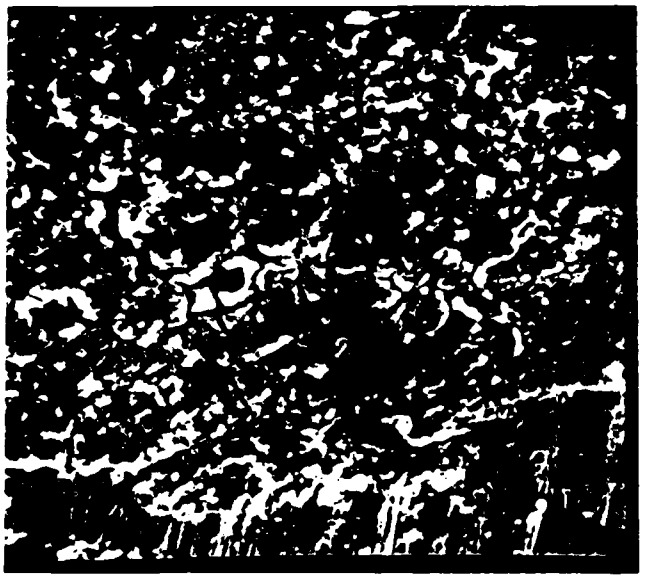

1000X

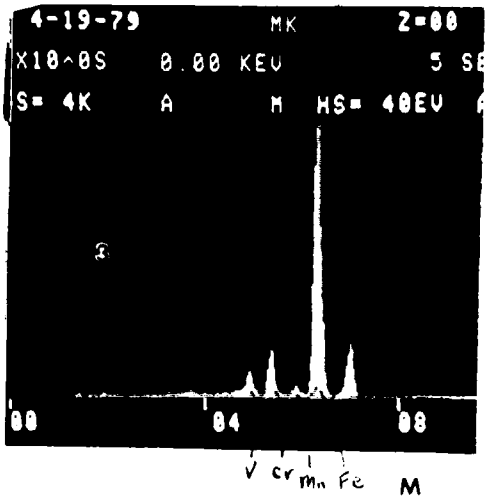

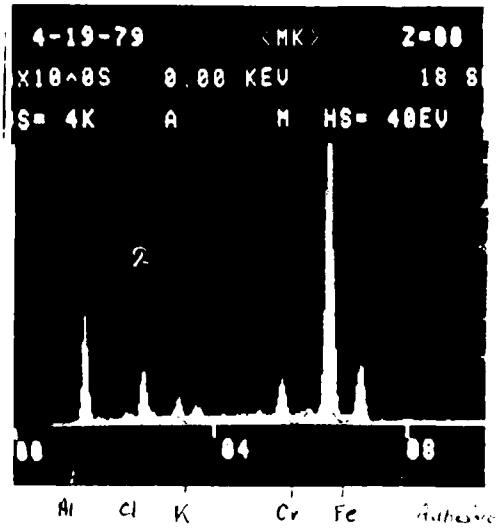

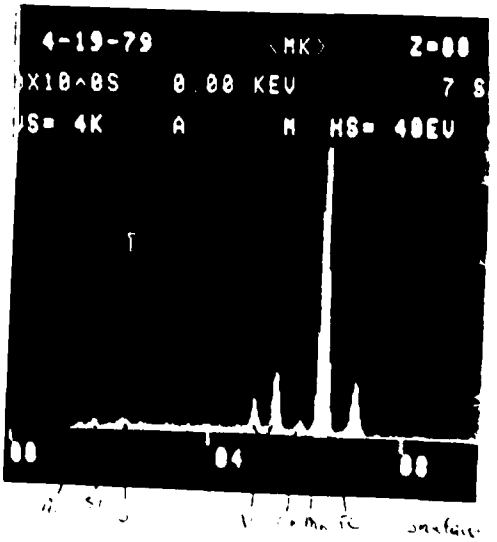

Figure 6. Scanning micrographs and EDAX analysis of the outer surface of piece D. The analysis shows the adhesive layer to contain almost no vanadium in contrast to the composition of the spacer material which contains reasonable amount of vanadium. It must be noticed that the rotor material contains negligible vanadium.

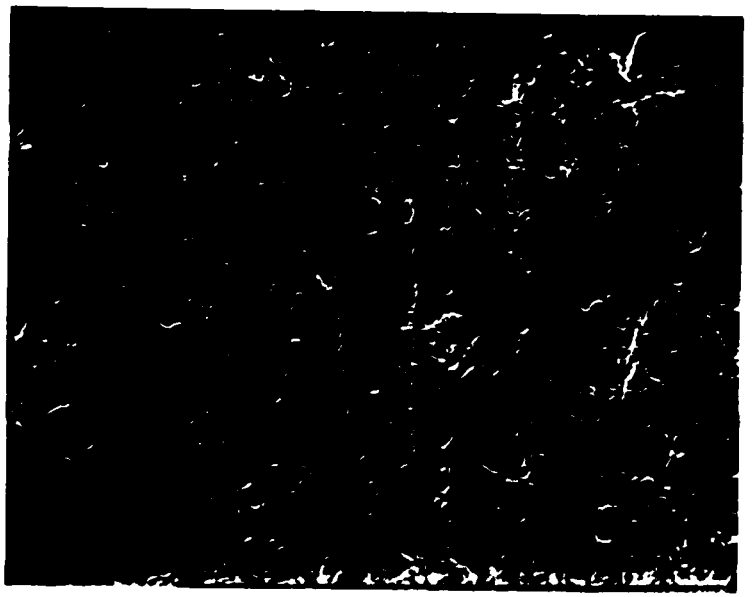

50

500X

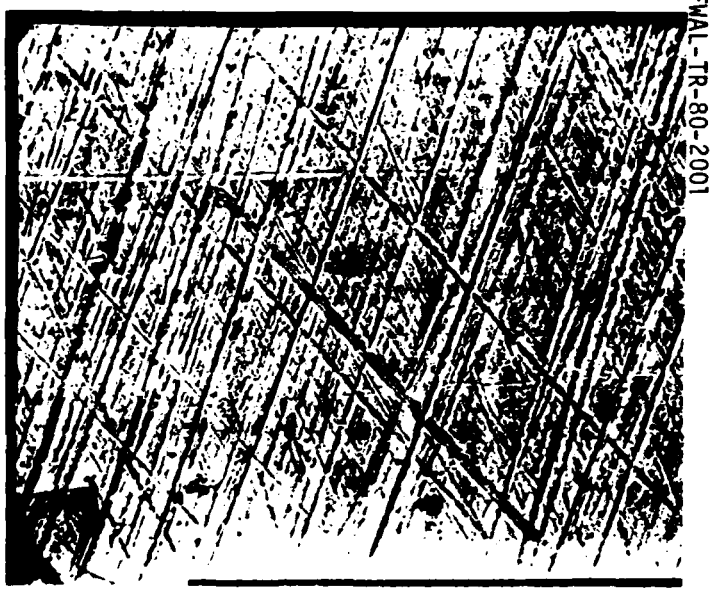

500X

Figure 7. Areas on the inner surface of the failed pin spacer parts, showing no presence of cracks. However the surface shows extensive surface damage in the form of scoring, spalling and surface pitting resulting from both abrasive wear (during testing) and poor machining during fabrication.

200X

500X

Figure-8. An example of the inner surface of those pin-spacers which passed the life test with no failure. Brinelling or surface indentations are observed, probably caused by debris formed from the contacting surfaces during testing. The extent of damage observed here is far less than that of the failed spacer inner surface.

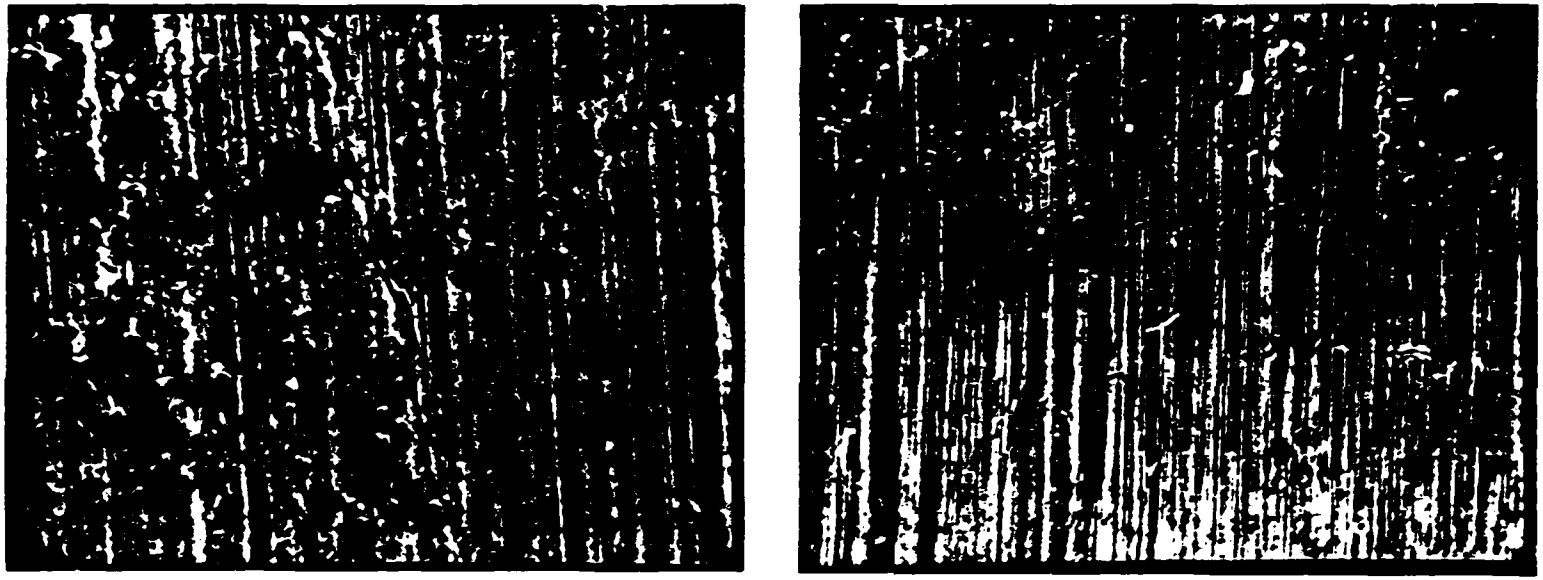

500X 200X

Figure 9. Outer surface of the pin-surface which did not fail during the life test, showing less extensive abrasive wear damage, smaller number of cracks compared to those found on the failed space surface. In addition there is no evidence of the presence of trapped particles or debris on the surface.

100X

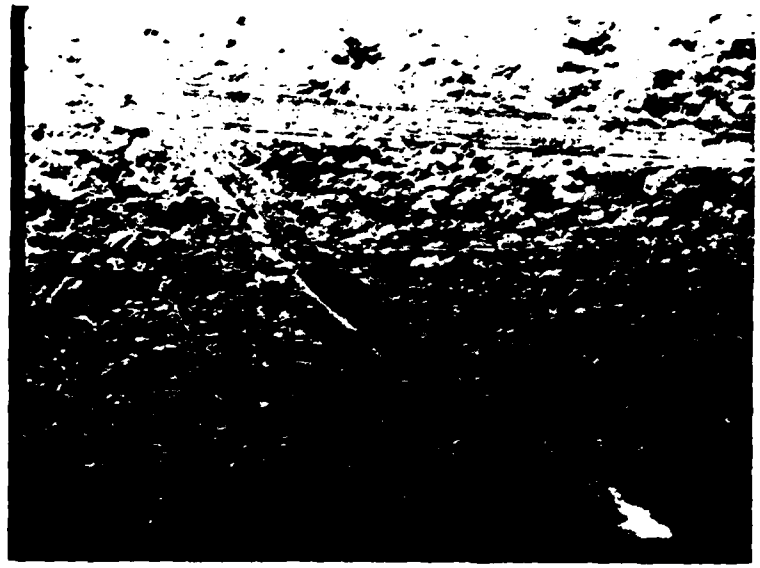

100X

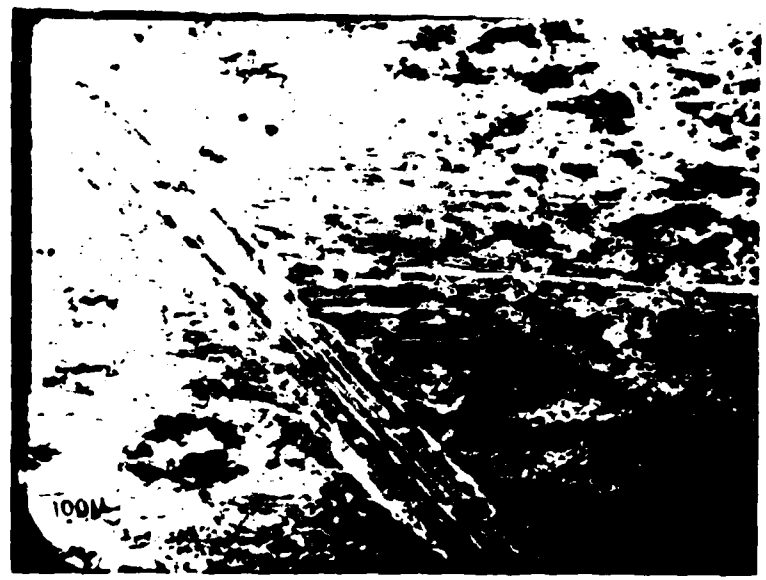

200X

Figure 10. Scanning micrographs of the outer surface of the Dynavector pin which had a diameter ~ 0.179 in. (spec. requires a diameter of 0.165 to 0.175 in.), showing some evidence of abrasive wear, however no debris, asperities were found.

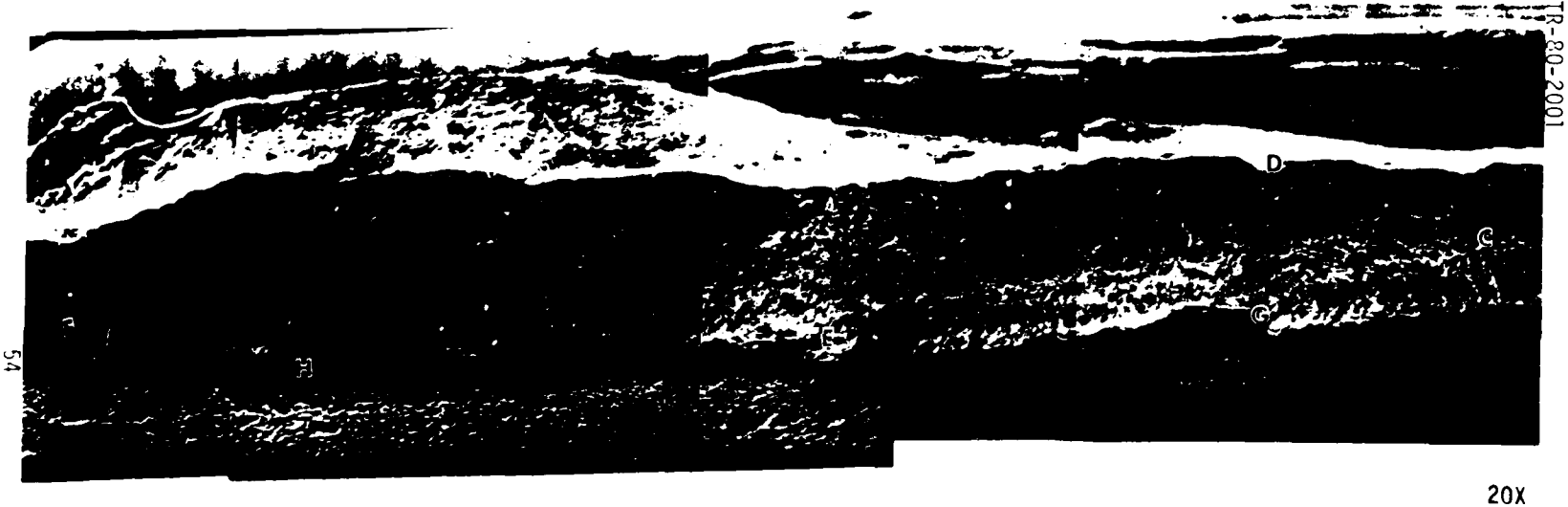

Figure 11. Scanning micrographs of the fracture surface #1 (see Fig. 1) of spacer piece A, showing multiple crack origination and initial propagation sites (see A, B, C, D, E, G, H) mostly from the outer surface of the pin spacer (see Fig. 2). River patterns (at E, F and C) indicate the fracture path advanced from left to right almost parrallel to the pin spacer axis.

1000X

Area B (Fig 11) showing the appearance of quasi-cleavage facet separations with an abrupt change in river patterns; an indication of lack of material ductility.

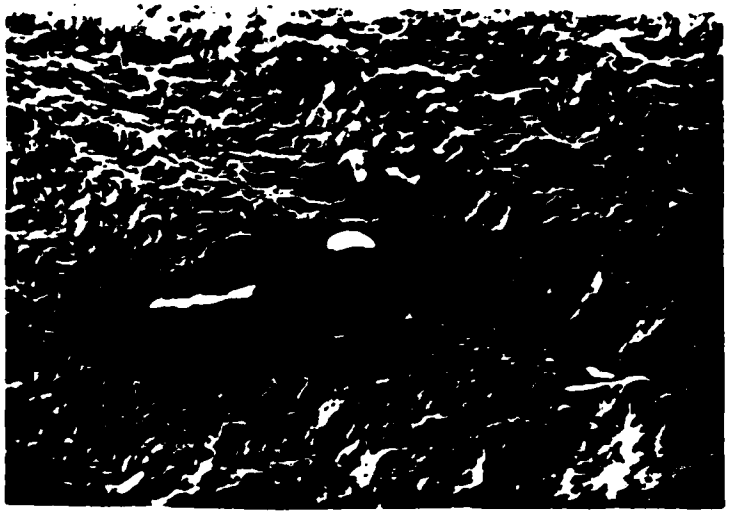

200X

Area C (Fig. 11) showing fatigue striations, areas damaged by rubbing and deep secondary cracks running longitudinally through the fracture surface (at 1)

Area D (Fig. 11) showing the appearance of fast brittle fracture (coarse striations) with many cracks running perpendicular to the surface.

200X

Coarse cleavage type steps.

50X

one of the crack initiation sites near G (Fig. 11) from the outer surface of the spacer with the direction of the crack propagation indicated by arrows.

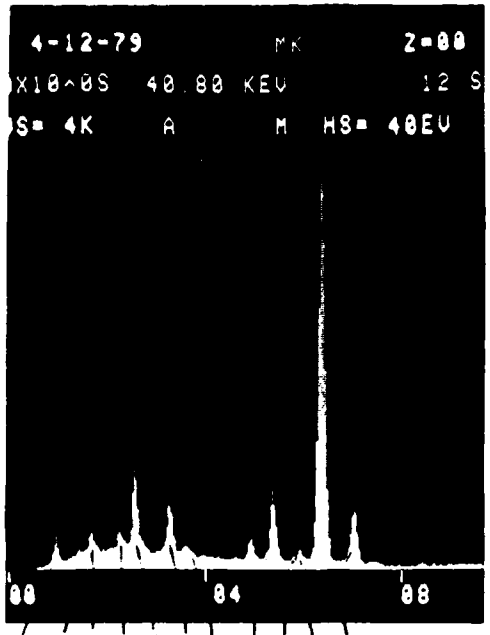

EDAX of the spacer inner wall shows no evidence of foreign material

Figure 12 Cont'd

Inner wall of the failed spacer piece A, showing abrasive wear (scars) markings, both radial and axial near 1 and 2, along with surface pits and some debris particles (or chips).

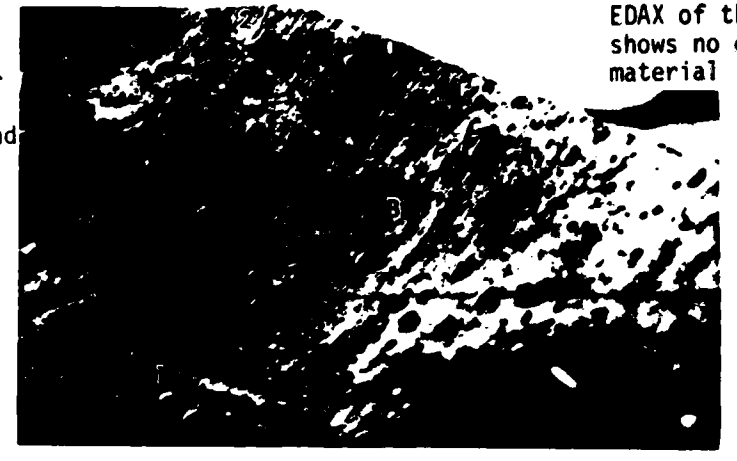

100X

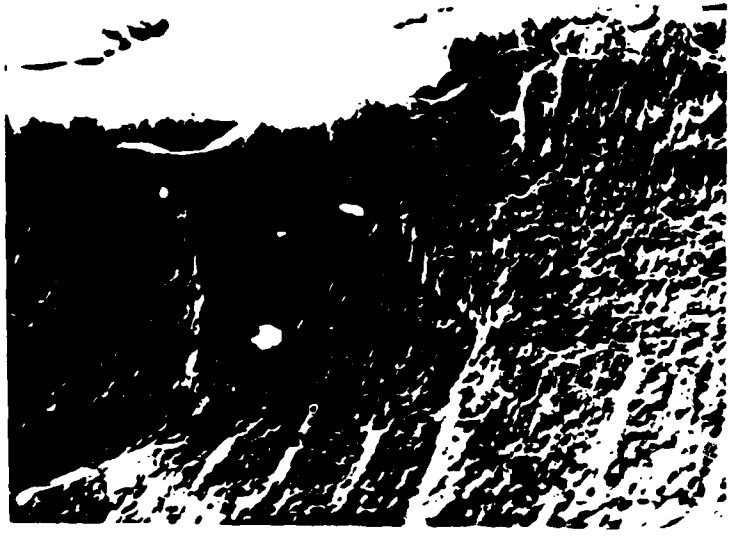

100X

Area F (Fig. 11) showing early stages of fatigue crack growth (fine striation at 1) both radially and longitudinally. Observed cracks show that the material was highly stressed and is brittle.

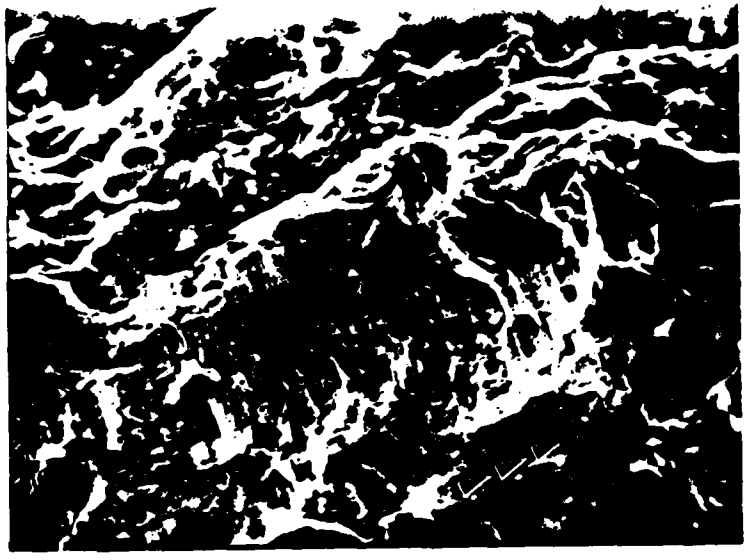

2000X

Area E (Fig. 11) showing fatigue crack propagation from the spacer outer surface. (see arrow)

Figure 12. Different areas on the fracture surface 1 of piece A.

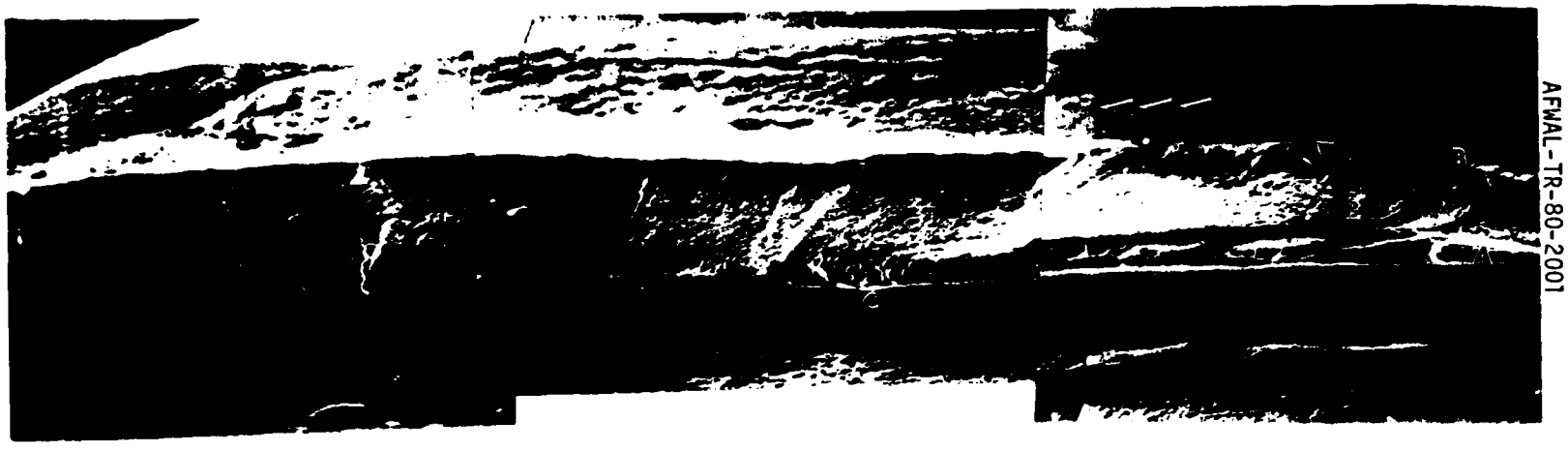

Fracture surface 2 (Fig. 1) showing fast fracture advancing from right to left (arrow).

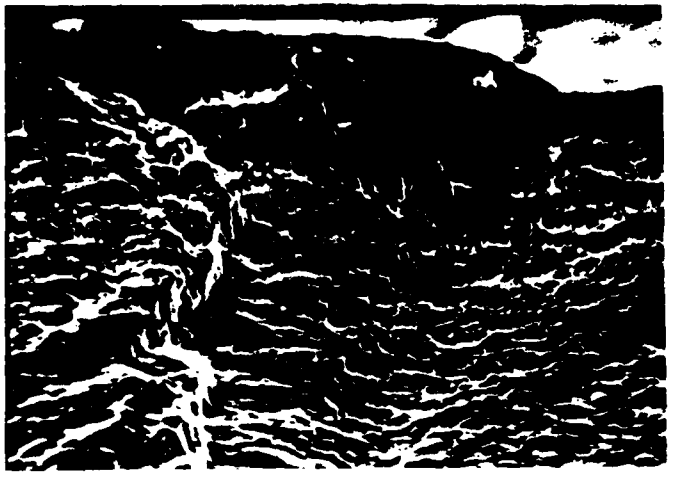

Fracture zone near B above showing closely spaced striations, indicating early stages of crack propagation (low fatique cycles)

Figure 13.

Fracture surface of piece D of the failed spacer

20X

500X

Area near B above showing fatigue crack initiation and propagation zone

200X

Area near A above (final structure)

Figure 14.

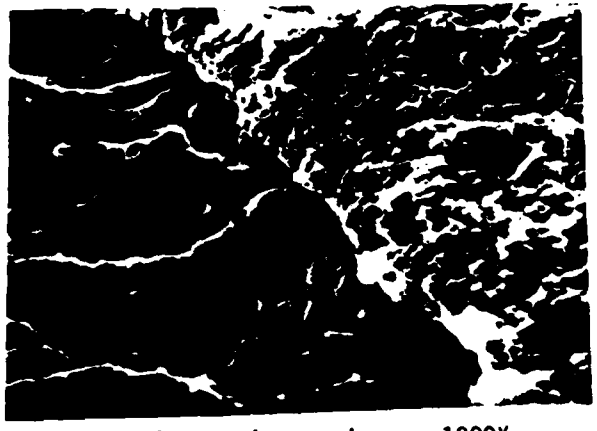

Area near C, showing region of fatigue crack propagation (extensively rubbed areas) next to final failure (separation area). 1000X

Area near D (above) showing a crack extending from the outer surface of the spacer into the surface. 100X

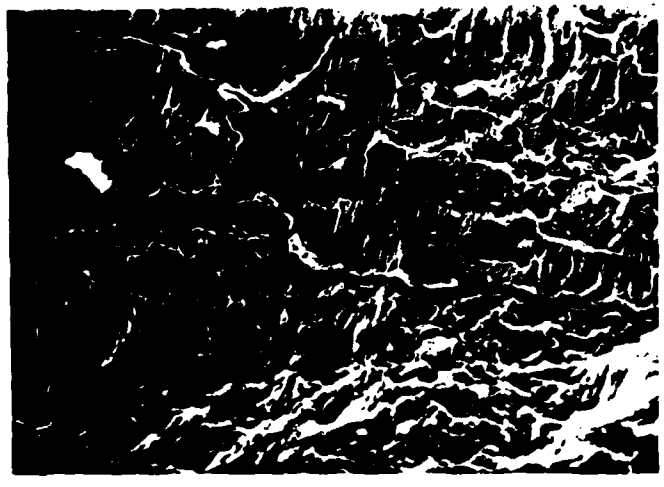

500X

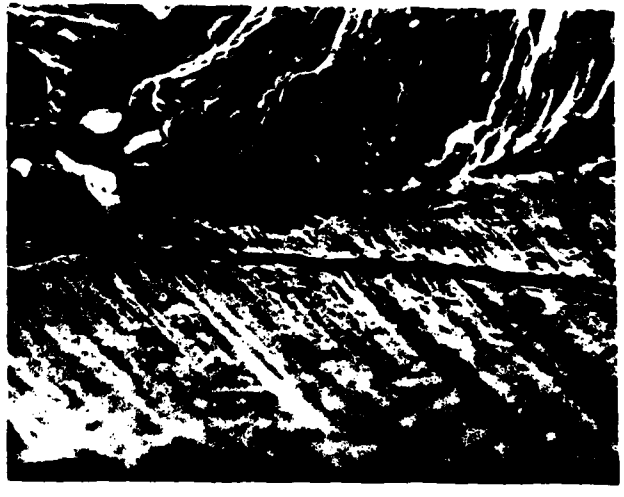

1000X

Area near above crack, enlarged.

Figure 14. Fracture surface of piece B showing the presence of deep secondary cracks, extensively rubbed areas during fatigue and multiple crack initiation sites; crack propagation indicated by arrows Lower surface near E shows what appears to be originally separated surfaces at high stress concentration sites, resulting from uncareful machining and poor surface finish.

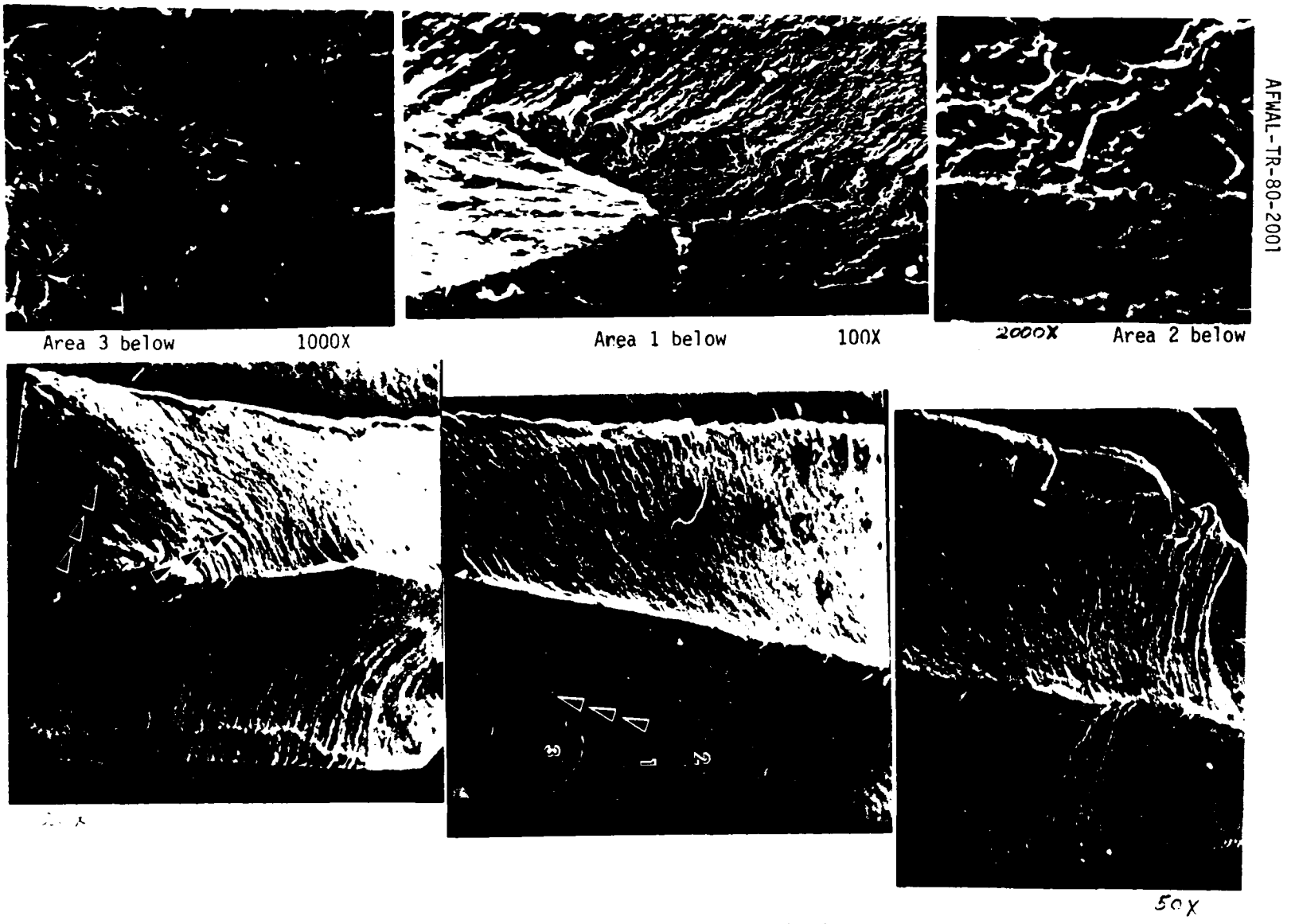

Figure 15. Fracture surface of piece C of the failed spacer showing zones of crack initiation and propagation (arrows).

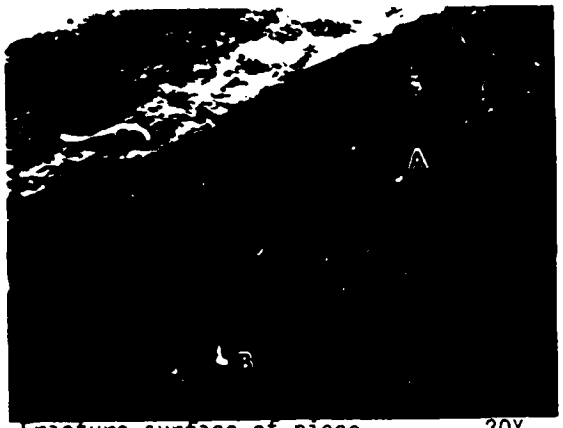

Fracture surface of piece 20X

bottom side of fracture near B 500X showing fatigue markings at 1, and cracking along that side produced possibly at high stress concentration due to poor machining.

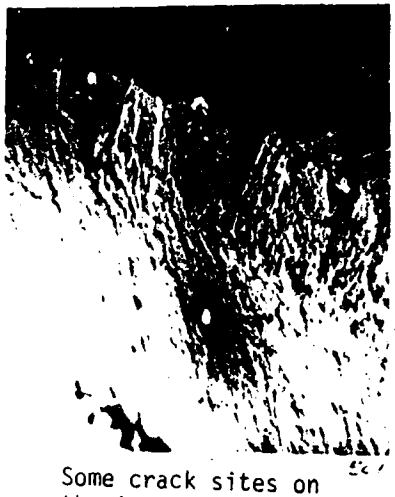

Some crack sites on the inner wall of the spacer as a result of poor machining

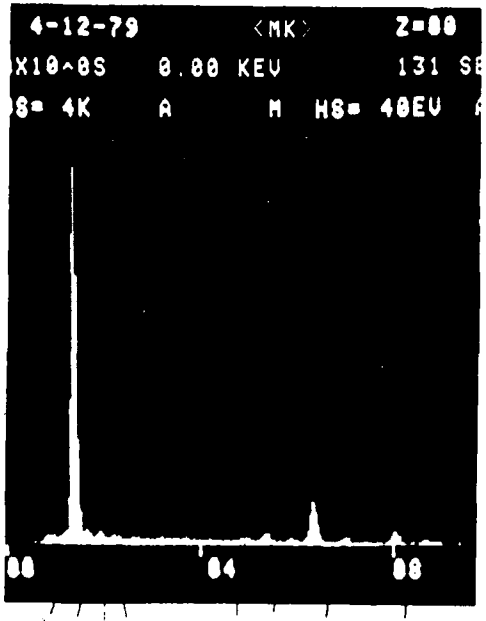

EDAX of area C, showing abnormal high content of Al which might have added to weakening of those areas

Area near A (above)

Figure 16. Fracture surface of piece D of the failed pin spacer.

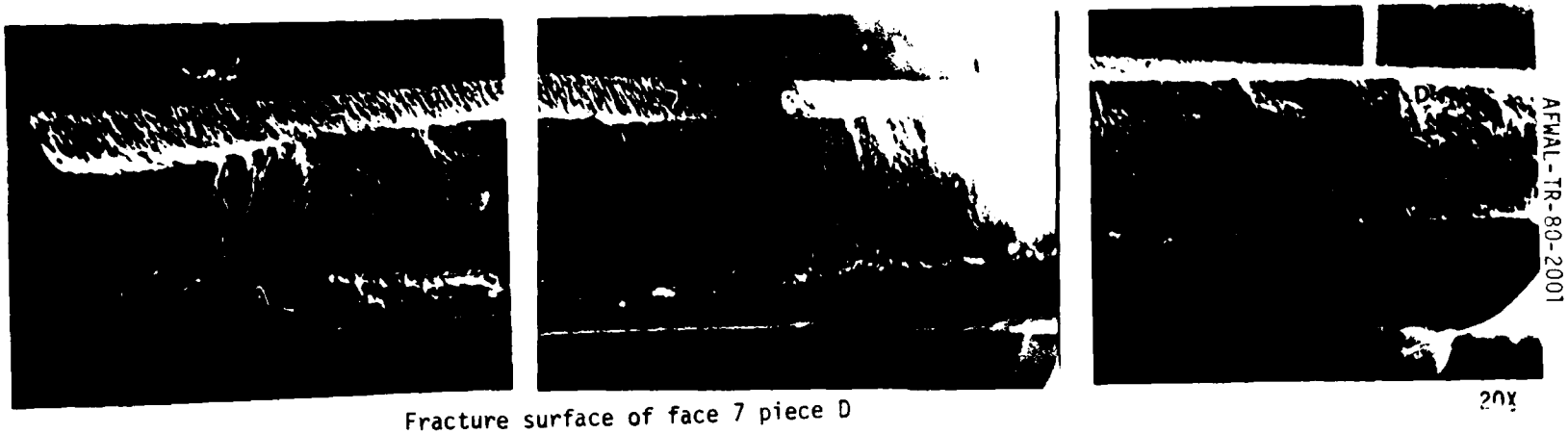

Fracture surface of face 7 piece D

50X

Area near A above

200X

Area C (left) enlarged

500X

Crack at B (left)

Figure 17. Scanning micrographs of piece D of the failed spacer, showing deep crack at the outer surface (arrow points towards the relative sliding direction of rotor w.r.to spacer as seen from the shape of the crack); crack initiation sites exist along the edge of the fracture surface (see eg. A, C)

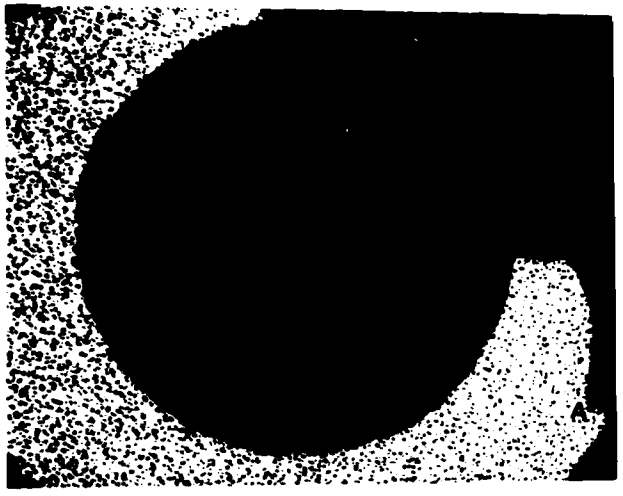

20X

Cross section of piece B
(Fig. 1) of failed pin spacer

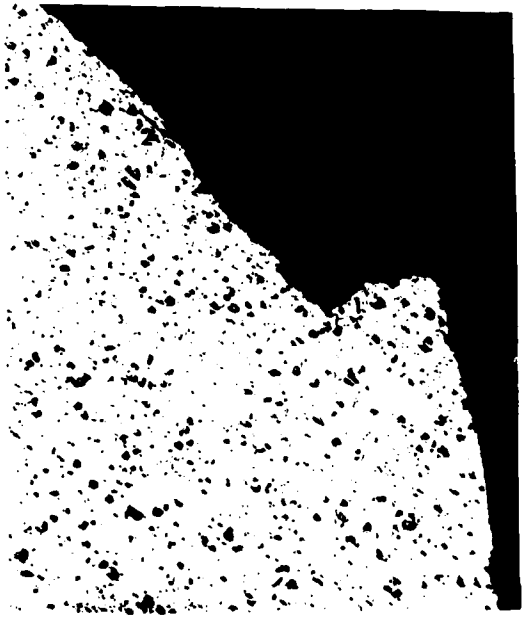

100X

Area near A enlarged showing small cracks 1, 2 propagating from the outer surface of the spacer.

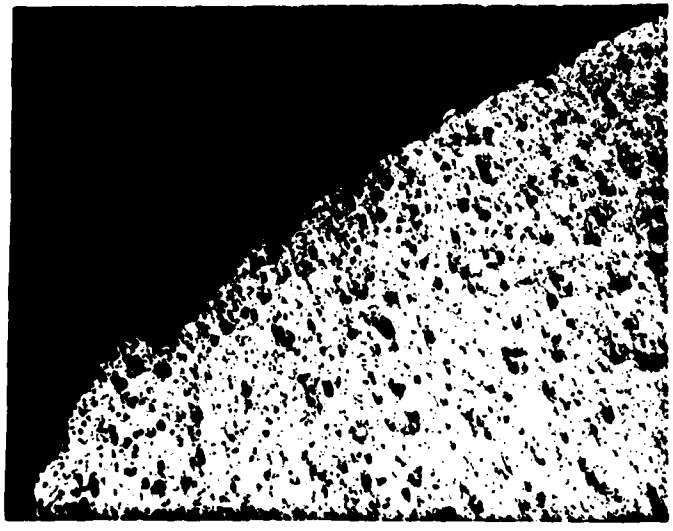

Area near B enlarged, showing cracks at the outer spacer surface (at 3, 4)

Area of crack 3 enlarged

500X

Figure 18

100X

500X

Areas along the outer surface of the failed pin spacer (cross section as polished), showing cracks propagating from the outer surface inwards and branching.

Figure 18. con't Cross section of Part B of the failed pin-spacer, showing a large number of secondary cracks originating from or near the outer surface of the spacer.

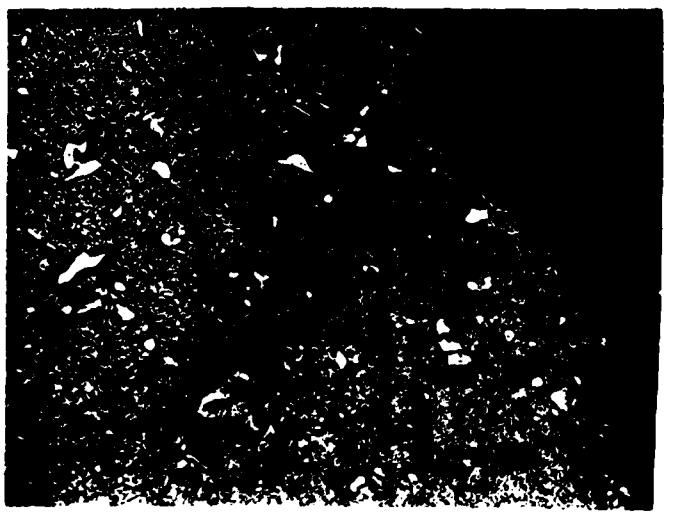

above section after etching showing no evidence of microstructural defects.

500X

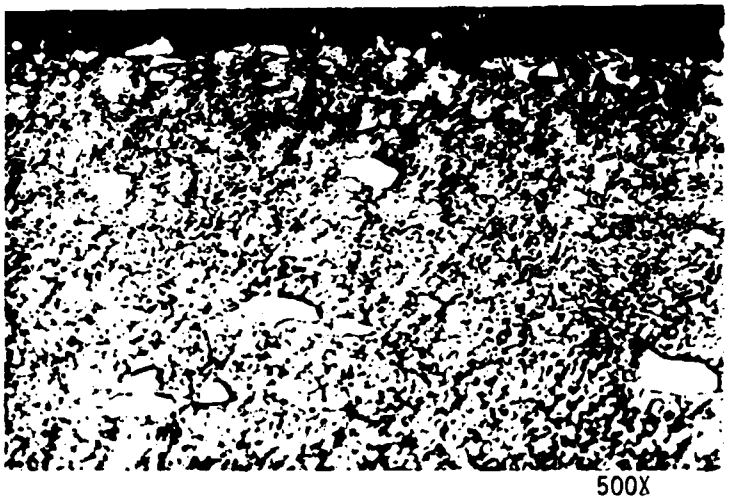

500X

Longitudinal section through the failed spacer outer surface, showing additonal cracks beneath the fracture surface. No microstructure defects, inclusions or inhomogeneities are observed. No decarburization has occured.

200X

Inner surface of the spacer after etching (longitudinal section) showing some worn type areas (along AA) due to abrasive wear action by existing debris and particles.

Figure 19. Microstructure of the pin-spacer piece B which failed during the life test.

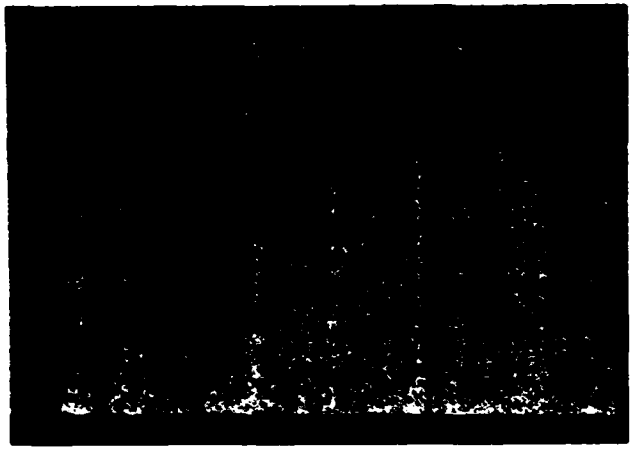

I.D.

O.D.

50X

longitudinal section in the spacer

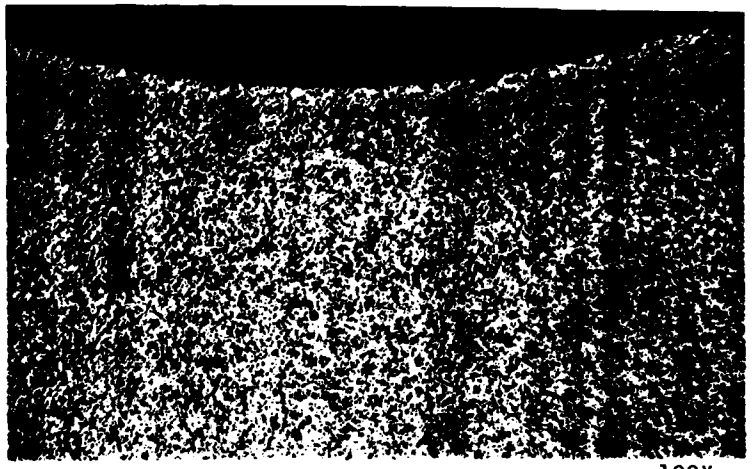

I.D.

100X

cross section of the spacer

Polished sections of a spacer which passed the life test with no failure, showing no cracks.

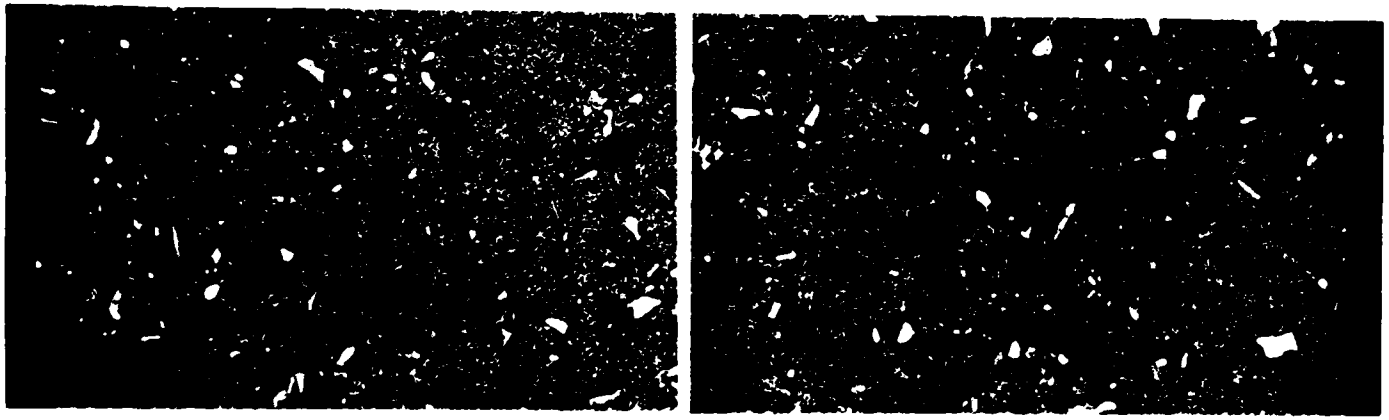

O.D.

I.D.

- Figure 20. cross section of the spacer as etched, showing a uniform microstructure with no visible cracks.

I.D. : inner diameter
O.D. : outer diameter

ID

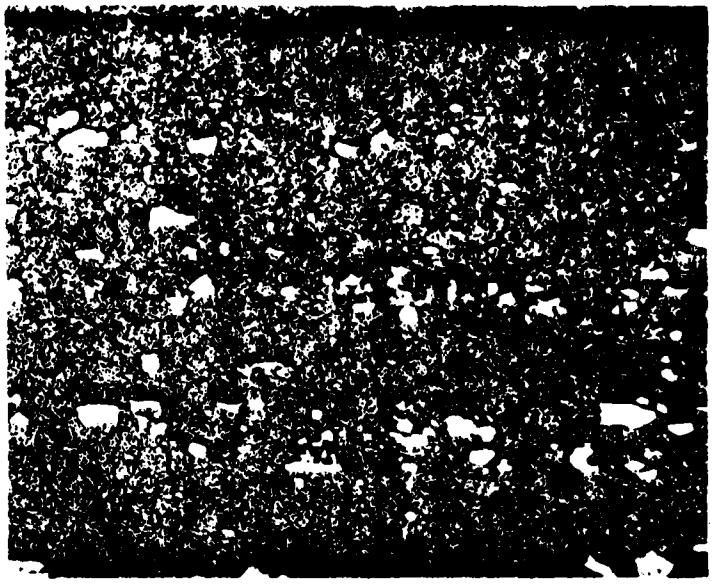

500X

Longitudinal section through a pin spacer which did not fail during the life test, showing neither metallurgical nor manufacturing defect.

OD

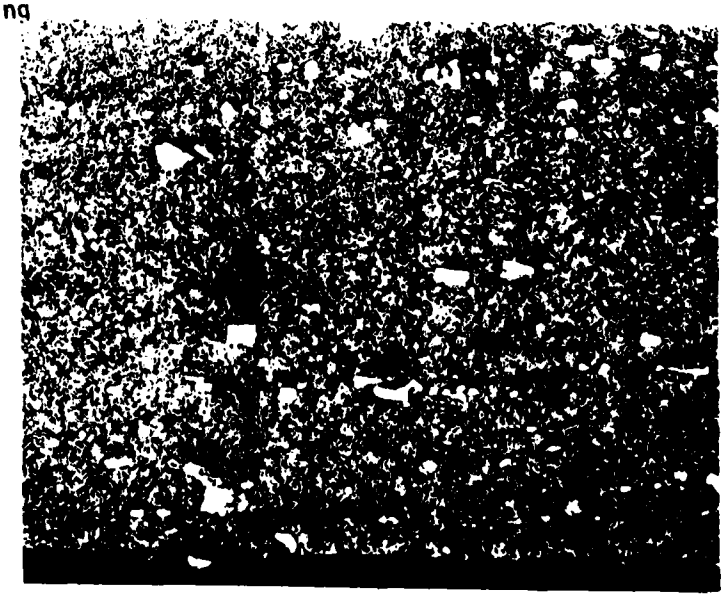

500X

Figure 20 con't. Longitudinal and cross sections through one of the provided pin-spacers which sustained the life test with no failure.

*U.S.Government Printing Office: 1980 — 657-084/771


DA
FILM
9-